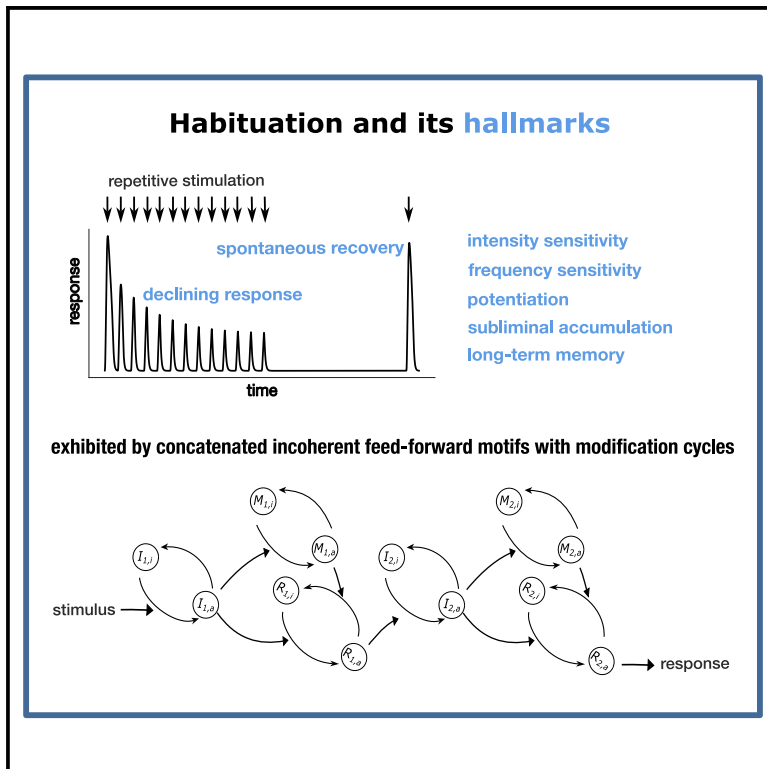


Biochemically plausible models of habituation for single-cell learning

Graphical abstract



Authors

Lina Eckert, Maria Sol Vidal-Saez, Ziyuan Zhao, Jordi Garcia-Ojalvo, Rosa Martinez-Corral, Jeremy Gunawardena

Correspondence

rosa.martinez@crg.eu (R.M.-C.), jeremy_gunawardena@hms.harvard.edu (J.G.)

In brief

Eckert et al. study mathematical models of habituation, the simplest learning behavior, in single cells. They find that biochemically plausible networks based on negative feedback or incoherent feedforward motifs satisfy all single-stimulus hallmarks of habituation, as codified in animals with brains.

Highlights

- Habituation is a form of learning characterized by specific hallmarks
- Biochemically plausible models exhibit all single-stimulus hallmarks
- Timescale separation and reversal behavior underlie the hallmarks
- Models reconcile opposing views from neuroscience and cognitive science

Article

Biochemically plausible models of habituation for single-cell learning

Lina Eckert,^{1,2,5} Maria Sol Vidal-Saez,^{3,5} Ziyuan Zhao,^{1,5} Jordi Garcia-Ojalvo,³ Rosa Martinez-Corral,^{1,4,*} and Jeremy Gunawardena^{1,6,*}

¹Department of Systems Biology, Harvard Medical School, Boston, MA 02115, USA

²Max-Planck Institute for Neurobiology of Behavior, Bonn 53175, Germany

³Department of Medicine and Life Sciences, Universitat Pompeu Fabra, C/Dr Aiguader 88, Barcelona 08003, Spain

⁴CRG (Barcelona Collaboratorium for Modelling and Predictive Biology), C/Dr Aiguader 88, Barcelona 08003, Spain

⁵These authors contributed equally

⁶Lead contact

*Correspondence: rosa.martinez@crg.eu (R.M.-C.), jeremy_gunawardena@hms.harvard.edu (J.G.)

<https://doi.org/10.1016/j.cub.2024.10.041>

SUMMARY

The ability to learn is typically attributed to animals with brains. However, the apparently simplest form of learning, habituation, in which a steadily decreasing response is exhibited to a repeated stimulus, is found not only in animals but also in single-cell organisms and individual mammalian cells. Habituation has been codified from studies in both invertebrate and vertebrate animals as having ten characteristic hallmarks, seven of which involve a single stimulus. Here, we show by mathematical modeling that simple molecular networks, based on plausible biochemistry with common motifs of negative feedback and incoherent feedforward, can robustly exhibit all single-stimulus hallmarks. The models reveal how the hallmarks arise from underlying properties of timescale separation and reversal behavior of memory variables, and they reconcile opposing views of frequency and intensity sensitivity expressed within the neuroscience and cognitive science traditions. Our results suggest that individual cells may exhibit habituation behavior as rich as that which has been codified in multi-cellular animals with central nervous systems and that the relative simplicity of the biomolecular level may enhance our understanding of the mechanisms of learning.

INTRODUCTION

Habituation is considered to be one of the simplest and most universal forms of learning.¹ It is “non-associative” in requiring only a single stimulus, which elicits, upon repetitive presentation, a steadily declining response that reaches a plateau (Figure 1A). Such a change in response to the same stimulus is sometimes offered as an informal, lowest common denominator definition of learning. We habitually rely on habituation, in accommodating to ambient light or noise, and it occurs in a remarkably broad range of settings across the tree of life, from animals to plants,² plasmodial slime moulds³ and single-cell ciliates,⁴ and across different physiological scales, from the whole organism to tissues and individual cells.⁵ (The same word has also accrued different meanings: in plants, epigenetic “habituation” to hormone stimulation⁵ appears quite different to what is studied here.⁷) Habituation may be rationalized as a fundamental filtering mechanism, or regulator of attention, in systems exposed to multiple stimuli.^{8,9} Habituation of looking time has been widely used in studies of cognition in human infants,¹⁰ whereas a failure to habituate is associated with neuro-developmental deficits, such as autism spectrum disorder.¹¹

In a landmark study in 1966, Richard Thompson and Alden Spencer collated nine characteristic properties, or “hallmarks,” which had been repeatedly observed in studies of habituation

in vertebrate animals¹² (Table 1). These hallmarks go considerably further than merely ruling out receptor desensitization or effector fatigue, for which appropriate controls are necessary to ensure that habituation is really taking place. The hallmarks of “frequency sensitivity,” in which “more rapid habituation” occurs in response to faster stimulus repetition, along with more rapid spontaneous recovery (#4), and of “intensity sensitivity,” in which more rapid habituation occurs in response to less intense stimuli (#5), are especially noteworthy because they show that the underlying system is responding to multiple forms of information carried by the stimuli. The hallmarks reveal a rich complexity to habituation that lies beyond the simple depiction in Figure 1A.

Thompson and Spencer remarked on the agreement in their hallmarks across a wide array of responses and vertebrate species and made the influential suggestion that the hallmarks should be incorporated into the definition of habituation. Strikingly, these same hallmarks were also found when habituation began to be studied in invertebrate animals, as, for example, in Eric Kandel’s studies of learning in the marine snail *Aplysia*.¹³ In 2009, a special issue of the journal *Neurobiology of Learning and Memory* brought together experts from both sides of the animal kingdom to collate a refined and updated list of ten hallmarks that now form the basis for assessing habituation in animals¹⁴ (Table 1). The hallmarks in Table 1 are substantially

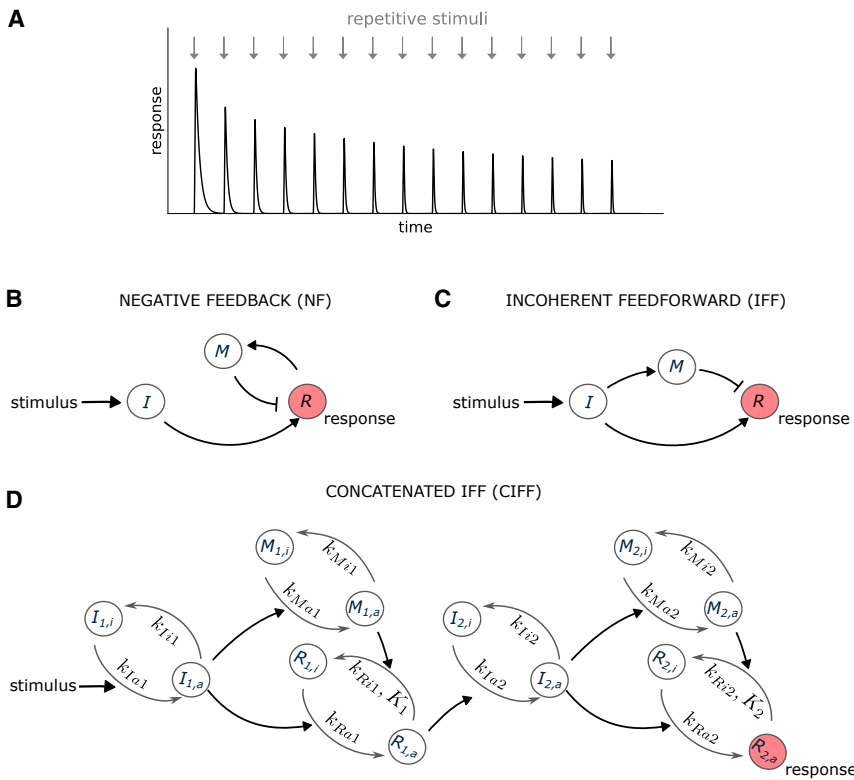


Figure 1. Habituation and networks for implementing it

(A) An illustration of a typical process of habituation, in which repetitive stimuli (arrows) elicit a steadily decreasing response that eventually reaches a plateau.

(B) Negative feedback (NF), in which the response activates the memory, which, in turn, inhibits the response. Nodes are denoted I for “input,” M for “memory,” and R for “response.” An arrow denotes a positive, increasing effect; a bar denotes a negative, decreasing effect.

(C) Incoherent feedforward (IFF), using the same notation as (B), in which the input activates both the response and the memory, but the memory inhibits the response.

(D) Concatenated IFF (CIFF) network, in which each node in (B) corresponds to a modification-demodification cycle. Subscript “i” denotes “inactive,” subscript “a” denotes active; an arrow that encourages activation is positive, whereas an arrow that encourages inactivation is negative. The labels on the edges give the model parameters, as explained in the text and the [STAR Methods](#). The parameters K_i on some inactivation edges are for the Michaelis-Menten formula that allows saturation. Numerical parameter values are given in [Table S1](#).

See also [Figure S7](#).

similar to those of Thompson and Spencer¹², with the addition of #10, on long-term habituation. Seven of the hallmarks (#1 to #6 and #10) require only a single stimulus, whereas the remaining three (#7 to #9) require multiple stimuli. We focus here on the former.

The hallmarks are not the whole story. They represent a perspective that comes largely from neuroscience. A rather different perspective on habituation, and on learning more generally, has emerged within cognitive science and takes issue with the findings of Thompson and colleagues.¹⁵ We are conscious of being outsiders in a complex debate with intellectual, historical, and sociological dimensions to which we can hardly do justice here. We defer further explanation to the [discussion](#), but note that our results appear to reconcile some of the differences.

Surprisingly, in view of the universality of habituation, the hallmarks have been less well studied outside the animal kingdom. This may reflect the long-standing debate as to whether complex behaviors such as learning are found there.¹⁶ It is only recently that the widespread consensus against this possibility has been reconsidered,^{17,18} and the possibility of cellular learning has started to emerge.^{19–22} Interestingly, sensitization, the counterpart of habituation ([discussion](#)), in which an increasing response is elicited to repetitive stimulation, has recently been discovered at the cellular level in both the innate immune system²³ and epithelial tissues.²⁴

The question of habituation in single cells is particularly significant. Because the underlying mechanisms must be very different from those found in animals with central nervous systems, it is especially interesting to know if, despite such marked

differences in implementation, the same hallmarks are nevertheless conserved. This would suggest that the hallmarks are essential features of the underlying information processing that gives rise to habituation, which may help, in turn, to characterize that information processing.⁹ Habituation is now well attested in single-cell ciliates,^{4,25,26} although few of the hallmarks have been assessed in this context. In a series of papers in the 1990s, starting with McFadden et al.,⁵ Dan Koshland showed in mammalian PC12 cells that noradrenaline secretion habituated to several chemical stimuli. Frequency sensitivity (but without testing the speed of spontaneous recovery), intensity sensitivity, and some other hallmarks were found to hold ([discussion](#)). Koshland’s work had almost no impact at the time, perhaps because of the negative consensus mentioned above. Nevertheless, it indicates that even cells which are not themselves organisms may still need to invoke habituation to address the information processing demands of a multi-cellular environment. (A more recent study considered some of the hallmarks of habituation in human embryonic kidney cells²⁷ but used a non-physiological stimulus. Habituation has also been shown in the slime mold *Physarum*,³ which is sometimes referred to as a single cell despite being a syncytium with multiple nuclei.)

As for the mechanisms underlying habituation, several models have been put forward—for a partial overview, see del Rosal et al.²⁸—but few of these seem appropriate for the biomolecular setting. The Russian psycho-physiologist Evgeny Sokolov was among those who developed the cognitive perspective of learning as the formation of an internal representation, or memory.²⁹ For habituation, such a memory could downregulate the

Table 1. The hallmarks of habituation

Number	Name	Description
1 ^a	habituation	repeated application of a stimulus results in a progressive decrease in some parameter of a response to an asymptotic level
2 ^a	spontaneous recovery	if the stimulus is withheld after response decrement, the response recovers at least partially over the observation time
3 ^a	potentiation of habituation	after multiple series of stimulus repetitions and spontaneous recoveries, the response decrement becomes successively more rapid and/or more pronounced
4 ^a	frequency sensitivity ^b	other things being equal, more frequent stimulation results in more rapid and/or more pronounced response decrement and more rapid spontaneous recovery (if the decrement has reached asymptotic levels)
5 ^a	intensity sensitivity	within a stimulus modality, the less intense the stimulus, the more rapid and/or more pronounced the behavioral response decrement; very intense stimuli may yield no significant observable response decrement
6 ^a	subliminal accumulation ^b	the effects of repeated stimulation may continue to accumulate even after the response has reached an asymptotic level [...]; this effect of stimulation beyond asymptotic levels can alter subsequent behavior, for example, by delaying the onset of spontaneous recovery
7	stimulus specificity ^b	within the same stimulus modality, the response decrement shows some stimulus specificity
8	dishabituation	presentation of a different stimulus results in an increase of the decremented response to the original stimulus
9	habituation of dishabituation	upon repeated application of the dishabituating stimulus, the amount of dishabituation produced decreases
10 ^a	long-term habituation	some stimulus repetition protocols may result in properties of the response decrement [...] that last hours, days, or weeks

Table adapted from Rankin et al.¹³

^aThe hallmarks investigated in this work.

^bWe have used our own names in this paper for these hallmarks. The hallmarks studied by Koshland in PC12 cells are described in [Table S5](#).

response to a repeatedly presented stimulus. In the molecular context of a cell, such a memory could build up in proportion to the response itself, which would be a negative feedback (NF, [Figure 1B](#)), or in proportion to the stimulus, which would be an incoherent feedforward (IFF, [Figure 1C](#)). The simplest implementations of these motifs would be the three-node networks shown in [Figures 1B and 1C](#).

NF and IFF are ubiquitous cellular motifs with distinctive properties.³⁰ Unlike most other motifs, they characteristically show adaptation: a sustained stimulus elicits a response peak that then decays to a lower steady state.^{31,32} The requirement for some form of response downregulation is common to both adaptation and habituation, which suggested that the NF and IFF motifs were good starting points for studying habituation. We found that they also have parameter regimes showing habituation, with many of the single-stimulus hallmarks,³³ but, crucially, we were unable to find regimes that exhibit frequency sensitivity. John Staddon, who was the first to develop mathematical models of habituation,^{34,35} made the important observation that serial linkage of motifs could give rise to frequency sensitivity ([Figure 4](#) in Staddon³⁴). Accordingly, we considered serially linked, concatenated networks built from the NF and IFF motifs. We also considered two other concatenated networks involving a receptor motif, which implements adaptation

through “state-dependent inactivation”³⁶; these other networks are discussed below.

Staddon was not thinking of the molecular realm and formulated his models in terms of physiological control theory using discrete, not continuous, time. He also did not examine other hallmarks. Recent work has considered some of the hallmarks more systematically but in terms of abstract models.^{28,37,38} Because such models are not biochemically based, it is hard to know what they tell us about the capabilities for habituation in single cells.

To address this problem, we considered molecular networks whose nodes are implemented by cycles of covalent modification and demodification, for example, through phosphorylation of a protein substrate by a protein kinase and dephosphorylation by a phospho-protein phosphatase. In the simplest case, individual substrate molecules are either modified or unmodified on a single site and the enzymes catalyze the conversion between these states. A classic analysis by Albert Goldbeter and Dan Koshland showed how such a cycle, far from being “futile,” as it was often described in the literature, enables the proportion of modified substrate to be sensitively regulated by the amounts and rates of the corresponding enzymes.³⁹ Modification-demodification cycles are ubiquitous in cellular signaling and have been widely studied as potential implementations of short-term

memory.^{40–43} Accordingly, we feel they are plausible biochemical primitives for implementing habituation. Modification is often unjustifiably regarded as the main actor in cell signaling but our treatment places modification and demodification on an equal footing.

We found that the cleanest behavior was exhibited by the concatenated IFF network (CIFF) in [Figure 1D](#). In this network, the nodes of the IFF in [Figure 1C](#) are modification-demodification cycles of different proteins, in which one of the protein substrate forms is considered “inactive” and the other “active.” The total number of molecules of each protein is kept constant and constitutes a separate “pool.” An arrow from a node to a transition signifies a positive effect on that transition, which may be activating because it increases the active form or inactivating because it increases the inactive form. We demonstrate that a region of parameter space may be identified in which this network robustly exhibits all seven of the single-stimulus hallmarks of habituation. The similar behavior of the other three networks is summarized below with details in the [supplemental information](#).

The motivation for this study of habituation was the rehabilitation of Herbert Spencer Jennings’ work on the avoidance hierarchy in the ciliate *Stentor roselii*,¹⁶ which prompted a reconsideration of learning in single cells.^{20,44} This paper brings together the cumulative contributions of Ziyuan Zhao’s unpublished undergraduate research project, Lina Eckert’s Master’s thesis³³ and part of Sol Vidal-Saez’s PhD thesis.⁴⁵ We examine the implications of our study for the question of single-cell learning in the [discussion](#).

RESULTS

The CIFF model with two concatenated IFF motifs

As discussed in the [introduction](#), we considered the concatenation of two IFF motifs ([Figure 1D](#)), each of which consists of an input (*I*) that receives a stimulus and activates a memory (*M*) and a response (*R*), which is deactivated by the memory. The response of the first motif is the stimulus for the second motif. We assumed that all biochemical reactions follow mass action kinetics, except for certain response deactivations, which we took to be saturated through a Michaelis-Menten type formula ([STAR Methods](#)). An enzyme typically exhibits a spectrum of rate behavior depending on its levels relative to its substrate.⁴⁶ At one extreme, with limited substrate, its rate increases linearly in the substrate concentration; at the other extreme, with abundant substrate, it exhibits saturation at a constant rate. In both cases the rate is also proportional to the enzyme concentration, which introduces nonlinearity ([STAR Methods](#)). We explored several options for where in the network the nonlinearity and the saturation should be placed, attempting to minimize the free parameters and settled on the choices in [Figure 1D](#). It would be interesting to know how the position and type of nonlinearity affect habituation, but this lies beyond the scope of this paper. The CIFF model is a nonlinear dynamical system with 14 parameters. We further assumed that the total concentration of each molecular species is 1, which sets the unit of concentration and also reduces the number of free parameters. We model the time evolution of the active proportion of each species using ordinary differential equations ([STAR Methods](#)). To examine habituation, the model is initiated in its basal steady state with all species in their inactive forms and is simulated with a

repetitive sequence of “rectangular” stimuli of period *T*, with *T*_{on} time units at amplitude *A* and *T* – *T*_{on} time units at amplitude 0 ([Figure 2A](#)). The unit of time is arbitrary, so that stimuli suitable for cell signaling, with *T*_{on} of tens of minutes,⁴⁷ may be represented. For the CIFF model, we took *T*_{on} = 1.11 throughout and altered only *T*. We considered habituation of the proportion of the response in the active state (“active fraction”) in the second IFF motif ($R_{2,a}/(R_{2,j} + R_{2,a})$) in [Figure 1D](#).

Measures of habituation and recovery time

In the light of hallmark #1 ([Table 1](#)), we assumed that the model had habituated when the relative change in the output after two consecutive stimuli was below a small threshold (which we chose to be 1%). The number of stimuli needed until that threshold was reached was taken as a measure of habituation time (denoted *ht*). In other words, if *p*_{*i*} denotes the peak height of the response to the *i*th stimulus, then *ht* = *i* when $(p_i - p_{i+1})/p_i < 0.01$ for the first time. We always measure habituation time in units of stimulus numbers, not absolute time, thereby avoiding any ambiguity when assessing frequency sensitivity, for which the inter-stimulus interval is changed. This method was followed by Thompson and Spencer in their original work¹² and has been widely used subsequently.^{5,25,26,48} Another measure used in the literature has been the decay rate, estimated by fitting an exponential to the response peaks. However, our models were sometimes best fitted to a sum of exponentials with different rates; therefore, we did not consider this method to be reliable.

For the recovery time (denoted *rt*), we followed the common experimental practice of measuring the time taken for the response to recover once stimulation stops. We simulated the model without any stimulus for some period following habituation and then applied a single test stimulus with the same shape of *A* and *T*_{on} as during habituation. We considered the system to have recovered when the response to the test stimulus was within a small threshold (which we chose to be 5%) of the response to the first pulse in the habituation protocol. We used a binary search algorithm to find the minimum time required for the response to reach this level and took that time as the definition of *rt*. Recovery time is measured in the unspecified (arbitrary) time units (“a.u.”) used in the model.

Principal hallmarks: Frequency and intensity sensitivity

By manually choosing parameter values and simulating the model as described above, we easily found parameter sets satisfying habituation and recovery (hallmarks #1 and #2). We did find parameter sets that showed intensity sensitivity (#5), but it was much harder to obtain frequency sensitivity (#4). We addressed this problem in several steps ([STAR Methods](#)). First, we developed an algorithm for assessing whether a simulation output reflects habituation. The algorithm extracts the sequence of peaks and troughs of the output as local maxima and minima of the trajectory and applies a filter of several conditions to the sequence to identify correctly habituating trajectories. Second, this algorithm was used to find parameter ranges that yield a 14-dimensional hypercube in parameter space ([Table S1](#)) in which habituation was typically observed. This parametric region was found by trial and error through iteratively growing each parameter range. Third, this region was used to run an

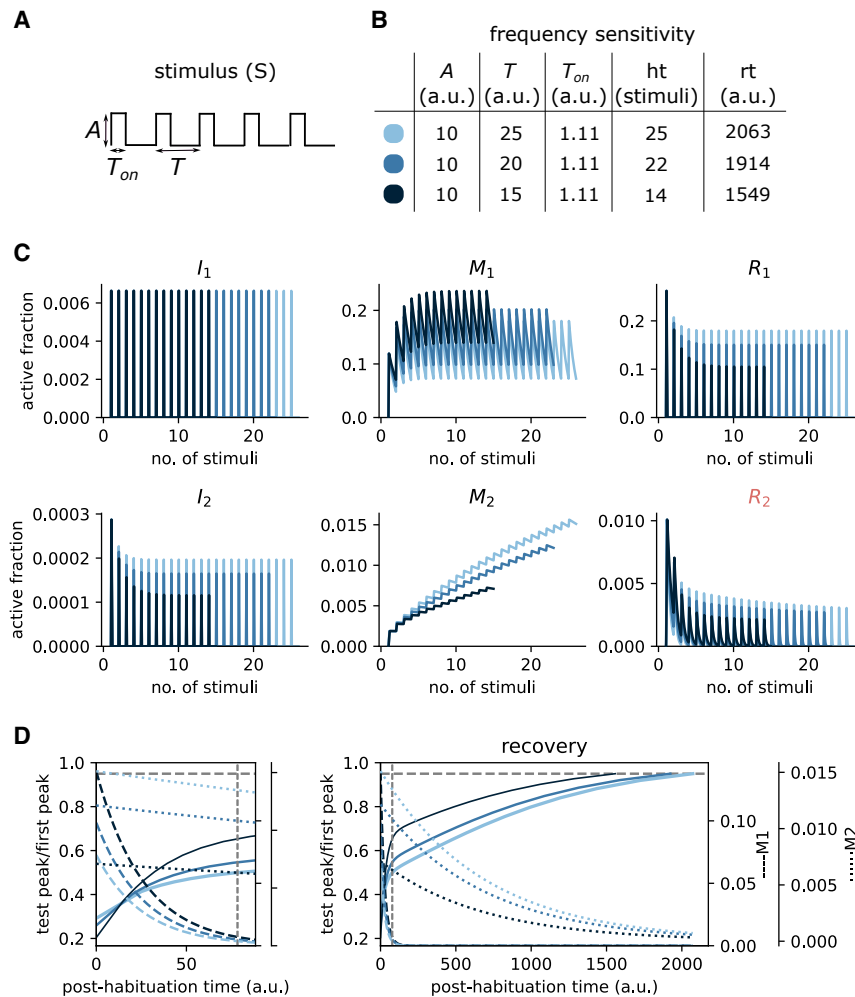


Figure 2. Frequency sensitivity for the CIFF model

The CIFF model is shown in Figure 1D.

(A) Schematic of the stimulation protocol.

(B) The table shows frequency sensitivity (hallmark #4) for the parameter values in Table S1, giving the habituation and recovery time for the three specified stimulation frequencies and the fixed amplitude.

(C) Dynamics in terms of stimulus number of the active fractions of each of the six variables in the model, following the color code in (B).

(D) Recovery behavior after habituation to a test stimulus at the post-habitation time shown on the horizontal axis. The plots give the active fraction of R_2 (solid lines, left-hand scale) at the peak of the response to a single test stimulus applied at the post-habitation time specified on the horizontal axis. These curves were smoothed by interpolation from the finite set of times at which the test stimulus was applied. The plots also show the active fractions of M_1 (dashed lines, first right-hand scale) and M_2 (dotted lines, second right-hand scale), measured in the simulation at the specified post-habitation time. Note that the curves for M_1 and M_2 are dynamical trajectories, whereas that for R_2 is a “response envelope.” The M_1 curves coincide in the main plot but are seen more clearly on a larger scale in the left-hand plot. The horizontal dashed line marks the recovery threshold of 95%. The vertical dashed line marks the time when M_1 has decreased by 95%; this line also marks the boundary between the fast and slow recovery regimes discussed in the text and visible in the main plot.

See also Figure S7 and Table S1.

evolutionary algorithm from the Paradiseo evolutionary-computation framework⁴⁹ that minimizes the cost function:

$$\frac{ht_1^f}{ht_2^f} + \frac{ht_2^f}{ht_3^f} + \frac{ht_1^A}{ht_2^A} + \frac{ht_2^A}{ht_3^A} \quad (\text{Equation 1})$$

Here, for each evaluated parameter set, ht_1^f , ht_2^f , and ht_3^f are the habituation times for three selected stimulation frequencies, $f_i = 1/T_i$ with $f_1 > f_2 > f_3$, respectively, at a fixed selected amplitude A , and ht_1^A , ht_2^A , and ht_3^A are the habituation times for three selected intensities $A_1 < A_2 < A_3$, respectively, at a fixed selected frequency. The selected amplitudes and frequencies are shown in Figures 2B and 3A. Frequency sensitivity requires that $ht_1^f < ht_2^f < ht_3^f$, so that the first two terms in Equation 1 would both be < 1 . Similarly, intensity sensitivity requires that $ht_1^A < ht_2^A < ht_3^A$, so that the last two terms of Equation 1 would also both be < 1 .

Minimization of Equation 1 does not guarantee that any of its terms will be < 1 nor would it rule out compensation between them, but in practice, we found low values for which all four terms were < 1 . We also did not test recovery times during optimization for efficiency reasons. As a final step, we tested the 20 parameter sets with the lowest cost-function values to check whether both

habituation time and recovery time behaved as expected for the frequency and intensity settings shown in Figures 2B and 3A. Of those parameter sets that passed this test, we reported the one with the lowest cost-function value in Figures 2B and 3A, with the corresponding parameter values given in Table S1. We further checked for this parameter set that habituation and recovery times were decreasing, not necessarily strictly, with increasing stimulation frequency at fixed intensity, for all integer values of T in the range shown in Figure 2B and also that these times were increasing, not necessarily strictly, with increasing intensity at fixed frequency, for all integer values of A in the range shown in Figure 3A. Although we cannot be certain by numerical simulation that the same behavior will be found for all intermediate values of frequency and intensity, these tests suggest that our results are robust. As a further check, we also carried out parameter sensitivity testing, which is reported below.

Figures 2C and 3B give the dynamics of each of the six active fractions and are very informative. Note first the marked distinction between the memory variables M_1 and M_2 under both frequency change and intensity change. This arises from the time-scale separation evident in the parameter values. The decay rate for M_1 ($k_{M1} = 0.0382$) is more than 20-fold higher than that for M_2 ($k_{M2} = 0.00147$). Accordingly, in this stimulation regime,

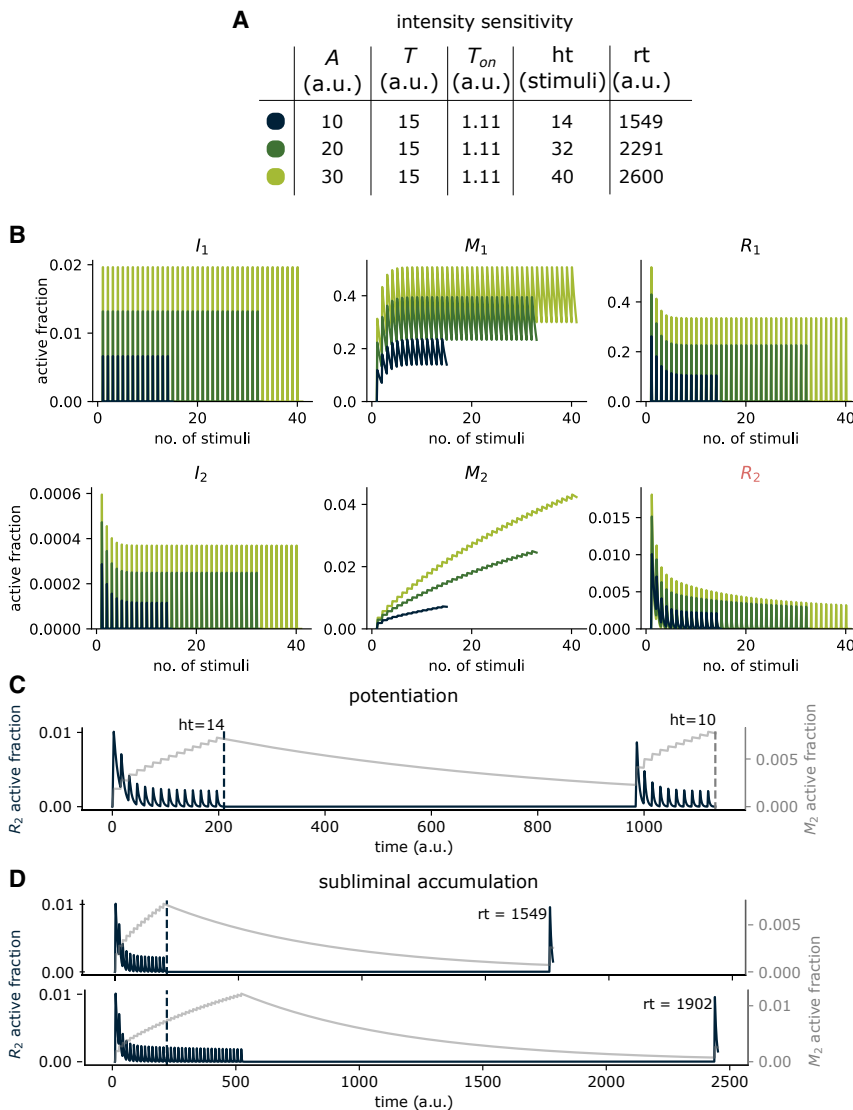


Figure 3. Intensity sensitivity, potentiation, and subliminal accumulation for the CIFF model

The CIFF model is shown in Figure 1D.

(A) The table shows intensity sensitivity (hallmark #5) for the parameter values in Table S1, giving the habituation and recovery time for the three specified stimulation intensities and the fixed frequency. (B) Dynamics in terms of stimulus number of the active fractions of each of the six variables in the model, following the color code in (A).

(C) Potentiation of habituation (hallmark #3). Active fractions of R_2 (dark blue curve, left-hand scale) and M_2 (gray curve, right-hand scale) are plotted during habituation, recovery for half the recovery time and rehabituation, for the habituation protocol coded dark blue in (A). Rehabituation yields faster habituation time, shown by the dashed vertical lines.

(D) Subliminal accumulation (hallmark #6). Plots of R_2 and M_2 as in (C), showing the effect of continuing stimulation beyond the habituation time (lower plot), which results in a longer recovery time compared with stopping stimulation immediately after habituation (upper plot).

See also Figure S7 and Table S1.

M_1 is largely driven by the stimulus and reaches saturation, whereas M_2 accumulates steadily. Second, M_1 and M_2 show opposite behavior under frequency increase at fixed intensity, with the former increasing and the latter decreasing (Figure 2C, middle plots). We refer to this as “reversal.” Reversal is not observed under intensity increase at fixed frequency, with M_1 and M_2 both increasing (Figure 3B, middle plots).

Reversal has interesting implications for the CIFF model. Under frequency increase at fixed intensity, I_1 remains constant, whereas the peak levels of M_1 increase. Within the first IFF motif, in which R_1 is activated by I_1 and deactivated by M_1 , and within this stimulation regime, this causes the peak levels of R_1 to decrease with increasing frequency (Figure 2C, top right plot). In contrast, under intensity increase at fixed frequency, the levels of I_1 increase along with the peak levels of M_1 . Within this stimulation regime, this causes R_1 to increase with increasing intensity (Figure 3B, top right plot). These differences in the output of the first motif are then propagated into the second IFF motif. With higher frequency at fixed intensity, R_2 is less activated by I_2 and

less inactivated by M_2 and habituates more quickly. Moreover, when the stimulus is withdrawn, M_2 is at a lower level at a higher frequency, so that it takes less time to decay, thereby resulting in a faster recovery time. With higher intensity at fixed frequency, the reverse happens: R_2 is more activated by I_2 and more inactivated by M_2 and thereby habituates more slowly. The higher levels of M_2 also cause slower recovery at higher intensity, although that has not been considered as an aspect of hallmark #5.

The two features of timescale separation and reversal behavior of the memory variables appear to be crucial for frequency and intensity sensitivity. We consistently found them for other parameter sets obtained from our optimization procedure (and also for other models, as reported below). Staddon originally attributed frequency sensitivity to timescale separation but had not appreciated the reversal feature. We reanalyzed Staddon’s discrete-time model and found that it also exhibited reversal behavior of the memory variables (data not shown).

Another notable feature of the dynamics, under both frequency and intensity change, is that R_1 also habituates. We therefore considered whether a single IFF motif could also exhibit the hallmarks of habituation. This was not the case. As with the CIFF model, habituation and recovery were easily found but, despite extensive parameter optimization, as described above, we only found parameter sets that showed weak intensity sensitivity without frequency sensitivity (data not shown).

whereas M_2 is largely constant (left-hand plot). Here, M_1 dominates the dynamics. The response to a post-habituation test during this period shows a sharply increasing recovery peak (main plot). Subsequently, M_1 has decayed to a negligible level, whereas M_2 continues its much slower decay (main plot). Here, M_2 dominates the dynamics and the response to a post-habituation test is a more slowly increasing recovery peak (main plot). Similar biphasic regimes in post-habituation recovery have been observed in experimental data, in *Aplysia* (Figure 2 in Pinsker et al.¹³) and in the single-cell ciliate, *Stentor coeruleus* (Figure 6 in Wood⁵⁰). Our results suggest that the underlying reason may also be timescale separation between memory variables, notwithstanding the substantial differences in the underlying mechanisms.

Remaining hallmarks: Potentiation, subliminal accumulation, and long-term habituation

As noted above, a striking feature of the CIFF model that helps explain frequency and intensity sensitivity is the timescale separation in the decay rates of the memory variables, M_1 and M_2 . M_2 decays far more slowly and therefore persists for much longer. This simple fact also accounts for the remaining single-stimulus hallmarks in Table 1, which we tested for exactly the same parameter values (Table S1).

For potentiation of habituation (hallmark #3), we habituated the system at each of the frequency and intensity settings in Figures 2B and 3A, allowed it to recover without stimulation for half the corresponding recovery time, and then applied for a second time the corresponding habituation protocol. In each case, we found that the system habituated more quickly, as exemplified in Figure 3C. As can be seen in the plot, M_2 has still not fully decayed when the second series of stimulations is applied, and this accounts for the faster habituation.

For subliminal accumulation (hallmark #6), we habituated the system, as for potentiation, at each of the frequency and intensity settings in Figures 2B and 3A, but, in each case, we continued the corresponding stimulation protocol beyond the habituation time until the relative change in the output after two consecutive stimuli had declined from the habituation threshold of 1% to 0.5%. We then determined the recovery time in the usual way, as explained above. In each case, we found that the recovery time was increased compared with stopping stimulation as soon as the system had habituated, as exemplified in Figure 3D. Here too, we see from the plot that M_2 continues to build up due to the continuing stimulation after the habituation time is reached, and this increase naturally leads to a longer recovery time.

The last hallmark in Table 1, of long-term habituation (hallmark #10), is the most ambiguous because neither the “properties” to be seen nor the question of how long is “long term” are made clear. One of the properties mentioned in Rankin et al.¹⁴ is “more rapid rehabilitation.” This makes it difficult to distinguish long-term habituation from potentiation of habituation (#3). Indeed, potentiation was regarded as an example of long-term memory by Koshland.⁵¹ What the CIFF model tells us is that there are, indeed, two timescales of memory. The slow decay and persistence of M_2 may continue well beyond the point at which the other variables, including M_1 , have relaxed back to zero. In consequence, the recovery time may be more than 10 times longer than the habituation time (Figures 2B and 3A). If

rehabilitation is attempted before the recovery time, then M_2 will still be present at some non-zero level, and rehabilitation will be more rapid (Figure 3C). Assuming more rapid habituation as the relevant property, the CIFF model may be said to exhibit hallmark #10. However, this is true for exactly the same reason that it exhibits hallmark #3.

In other literature on short- and long-term habituation, a more profound distinction has been made between memory that is encoded by post-translational modification (PTM) in the absence of protein synthesis, which may last for hours, and memory that is encoded by gene transcription and protein translation, which may last for days.⁵² The models presented here can say little about this kind of long-term memory. It is worth noting, however, that the NF and IFF motifs can be implemented by gene transcription and protein translation, rather than by PTM, and have similar properties.³² A model in which a second, or even a third, motif was of this form might correspond more closely to the biological context in which the long-term memory described in Goellet et al.⁵² has been found. This remains an interesting direction for future work.

Other models of habituation

We have shown that the CIFF model exhibits all seven single-stimulus hallmarks of habituation. We were therefore interested to know whether this could be replicated by other biochemically plausible models. The NF motif (Figure 1B) suggests one possibility, as noted in the introduction; therefore, we considered a concatenation of two NF motifs (concatenated NF [CNF], Figure 4A), in which, similar to the CIFF model, the nodes of the motifs correspond to modification-demodification cycles. We further reasoned that, in a single cell, stimulation would typically be detected by a cell-surface receptor.^{5,53} Certain receptor classes, such as receptor tyrosine kinases or G-protein-coupled receptors, respond to stimulation by post-translationally modifying themselves or accessory proteins.⁵⁴ In doing so, they can create refractory states, in which the receptor is neither activated nor can it respond to stimulation. Such a refractory state would act similar to an implicit NF because, as it builds up, it reduces the response to stimulation. This kind of state-dependent inactivation can give rise to adaptation,³⁶ which, as we noted in the introduction, shares common mechanistic features with habituation. Accordingly, we considered a receptor motif (P) consisting of a cycle of three states: P_i , which can respond to a stimulus and transitions to the active state, P_a , which transitions to the refractory state, P_r , which cannot respond to the stimulus and transitions back to P_i . We concatenated P to an IFF motif of modification-demodification cycles to form a RIFF model (Figure 4B). We further reasoned that cell-surface receptors also trigger cascades of downstream PTM, such as the highly conserved mitogen-activated protein (MAP) kinase cascades, which are known to be implicated in synaptic memory.⁵⁵ These cascades can feedback on the receptor to alter its behavior. Accordingly, we also considered a concatenation of P with a cascade of three modification-demodification cycles that negatively feeds back on P (R3MD, Figure 4C) to enhance entry to its refractory state. The R3MD model is different from the others in being cyclic.

It is interesting to reason about how these models might behave under repetitive stimulation, in the light of our findings for the CIFF model. If habituation were to be found, we expected

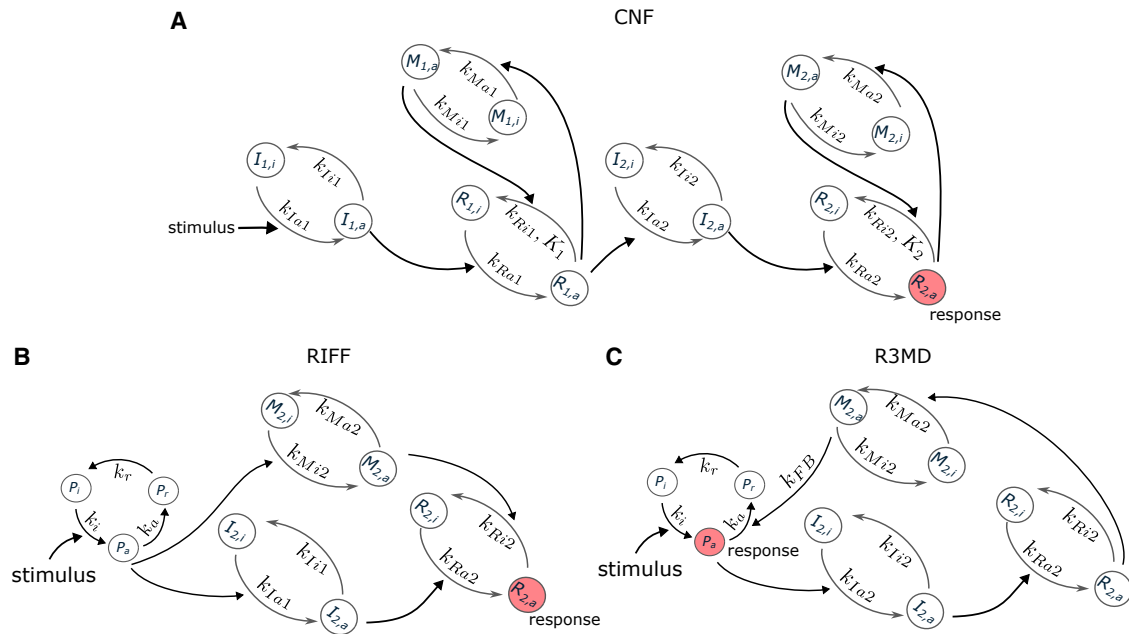


Figure 4. Other models that exhibit the hallmarks of habituation

(A) Concatenated NF (CNF) network, in which each node in Figure 1B corresponds to a modification-demodification cycle. See also Figures S1, S2, and S8 and Table S2.

(B) Receptor motif (P), consisting of a cycle of three states, as discussed in the text, concatenated to an IFF motif (RIFF). See also Figures S3, S4, and S9 and Table S3.

(C) Receptor motif (P), concatenated to a cascade of three modification-demodification cycles (R3MD) that negatively feeds back on the receptor. See also Figures S5, S6, and S10 and Table S4.

that the memory variables would act to reduce the response variables. These memories are denoted M in Figure 4. For the receptor-based models, the refractory state, P_r , acts implicitly to reduce the activated state of the receptor, which is the output to the second motif; therefore, we expected that P_r would also act as a memory variable. Because R3MD is cyclic, it was not immediately clear which variable should be considered as the response and expected to habituate. The activated state of the receptor, P_a , seemed like a reasonable guess because it connects P to the cascade. Here, both memory variables act to reduce P_a .

We subjected each of these three other models to the same process of evolutionary optimization described above for the CIFF model and were able to find in each case parameter sets that exhibited all seven of the single-stimulus hallmarks of habituation. The results are shown in Figures S1 and S2 (CNF), S3 and S4 (RIFF), and S5 and S6 (R3MD), with the corresponding parameter ranges and the parameter set with the lowest cost-function value shown in Tables S2 (CNF), S3 (RIFF), and S4 (R3MD). The memory variables were as we had predicted. Strikingly, the same crucial features of timescale separation and reversal for the memory variables, which we noted above for the CIFF model, were found to hold for all three models in Figure 4.

Robustness of the response

A single parameter set defines only one point in a high-dimensional parameter space. Because our results were found through random sampling, it is clear that the region of parameter space

that supports the hallmarks found here must necessarily contain an open subset of the high-dimensional space of parameters. If not, the probability of finding points in the region by sampling would be zero. This in itself is a sign of parametric robustness. However, it is not clear whether the region of parameter space is tiny or extensive nor what kind of shape it has. Such “parameter geography” is not straightforward to undertake in general. We therefore performed single-parameter sensitivity analysis by independently multiplying each parameter by 10^a , where a was drawn randomly from the uniform distribution on $[-1, 1]$, keeping all other parameters fixed at their identified values, and then testing for habituation with frequency and intensity sensitivity. These are the principal hallmarks from which the others follow, as noted above. The results are shown in Figures S7 (CIFF), S8 (CNF), S9 (RIFF), and S10 (R3MD). As expected for such analyses, some parameters had to be maintained within much smaller ranges than others. The CNF model had generally broader ranges and less disparity in ranges between parameters, whereas the RIFF model is much the opposite. However, all models exhibited reasonable robustness to parametric variation.

DISCUSSION

The question of learning outside of animals with brains has been fraught with controversy, which often appears, in historical perspective, to have been as much ideological as scientific.^{16,57,58} It is only recently that renewed interest in the question has arisen.^{17–22} Learning may occur at many biological scales,

but the cell is the unit of life, and we have focused here on habituation, typically regarded as the simplest form of learning, in single cells.

There is compelling experimental evidence for single-cell habituation in limited contexts. Habituation was well established many years ago in the ciliate *Stentor coeruleus* by David Wood,^{53,50} building on the pioneering work of Herbert Spencer Jennings,⁴ and these experiments have now been replicated with modern techniques by Wallace Marshall.²⁶ Because a single-cell organism must solve the same survival problems as any organism, in a world of “blooming, buzzing confusion,”⁵⁹ it may seem reasonable that evolution provided it with elementary forms of learning that are similar to those used by animals. Indeed, from an evolutionary perspective, we may even speculate that it was the former that gave rise to the latter.⁶⁰

Learning in single cells that are components of multi-cellular organisms is not obviously supported by this evolutionary rationale. Indeed, in adult animals, homeostasis is believed to maintain the constancy of the internal milieu, whereas the prevailing metaphor for animal development has been the operation of a program encoded in genomic DNA. The experiments undertaken in mammalian PC12 cells by Dan Koshland are therefore especially significant because they confirm habituation of noradrenaline secretion to multiple stimuli along with several of the hallmarks. Koshland's analysis was undertaken in full awareness of, and by analogy to, contemporary work on learning in animals. His earlier review of bacterial chemotaxis “in relation to neurobiology”⁶¹ ends with the declaration that “enzymology recapitulates neurobiology.” To our knowledge, Koshland's work has been the only systematic evaluation of habituation in single mammalian cells. In view of its importance and its subsequent invisibility in the literature, we have summarized this body of work in [Table S5](#), showing in which papers the evidence for the tested hallmarks may be found.

Koshland was a pioneer not only in studying habituation in single cells but also in bringing mathematical analysis to bear on biochemistry (as, for example, in Goldbeter et al.³⁹). It is surprising that his only published attempt to model habituation⁶² was limited to a scheme of receptor inactivation, resembling our P motif ([Figures 4B and 4C](#)) but without the state P_i . It is not difficult to see that this shows an exponentially declining response to repetitive stimulation, as in [Figure 1A](#). None of the other hallmarks were tested, nor would we expect, from our findings, that they would have been found (with the possible exception of recovery).

Koshland's model was limited, but it was grounded in the biochemistry and enzymology to which he himself had contributed. We have followed his example by formulating mathematical models built upon the biochemistry of PTM. The potential to modify the states of an individual protein molecule “on the fly,” as part of a cell's response to its environment, has always suggested substantial capabilities for information processing,⁴³ which have been strengthened by the links between PTM and short-term forms of memory.⁵² We have followed Koshland again in exploiting cycles of PTM and demodification, whose sensitivity properties he helped to explicate.³⁹ PTM cycles form the component nodes in the three motifs, NF, IFF, and P, which we have considered here.

The NF and IFF motifs ([Figures 1B and 1C](#)) characteristically arise in random sampling of small networks that exhibit adaptation.^{31,32} As mentioned in the [introduction](#), adaptation and habituation both rely on some form of response downregulation. The receptor motif, P, is also known to exhibit adaptation through state-dependent inactivation,³⁶ and, as we found, it too exhibits habituation (hallmark #1). This suggests that adaptation and habituation are related to each other, although no mathematical explanation has been found for such a relationship. The IFF and NF motifs exhibit several of the other hallmarks of habituation³³ (we did not test the P motif), but we were never able to find regimes that showed frequency sensitivity (#4). To address this, we have built on Staddon's insight into the impact of serial linkage³⁴ to analyze four concatenated models based on these motifs (CIFF, CNF, RIFF, and R3MD), which have yielded several interesting conclusions.

First, as just noted, although it is not difficult to show habituation (#1) and also recovery (#2), it is harder to show frequency sensitivity (#4). This suggests that merely exhibiting the declining response in [Figure 1A](#) should not be taken as adequate evidence of habituation. Many networks may show this behavior without having all the hallmarks. Second, the critical hallmarks appear to be frequency sensitivity (#4) and intensity sensitivity (#5). We had to use an evolutionary optimization algorithm to find parameter sets that satisfied these two hallmarks, but, once we had, the remaining hallmarks emerged for free, without the need for any further parameter searching. Third, the parameter optimization invariably leads to the distinctive properties of timescale separation and reversal. Each model has two memory variables. The decay time of one of them is much longer than that of the other (timescale separation), and they respond in opposite ways to increasing frequency at fixed intensity (reversal). This reversal is not seen with increasing intensity at fixed frequency. Staddon had noted the significance of timescale separation but not that of reversal, which, nevertheless, we found to also be true of his model.

It is striking that all our models exhibit both timescale separation and reversal, despite the corresponding parameter sets being found independently by a randomized search algorithm. This strongly suggests that they play a crucial role in giving rise to the hallmarks. In our models, they explain frequency and intensity sensitivity, whereas timescale separation, in the guise of the slow decay and persistence of the second memory variable, explains potentiation of habituation and subliminal accumulation (#3 and #6). Long-term habituation (#10) is more ambiguous, for reasons noted above. In our models, it occurs within the recovery time, where it is no different to potentiation. This suggests that the kinds of long-term memory that have been found experimentally, which can last for days,⁵² may reflect the biochemistry of transcription, translation, and epigenetics,⁶³ rather than that of signaling and PTM. If so, this may indicate a third timescale of habituation, beyond that which gives rise to potentiation. Models that can represent these other biochemical processes may help resolve this interesting point. We note, however, that there has been no experimental hint of a longer timescale of days in single cells.

Our results offer a partial strategy for experimental identification of molecular networks underlying proper habituation, in which the hallmarks in [Table 1](#) are satisfied. First, the relationship

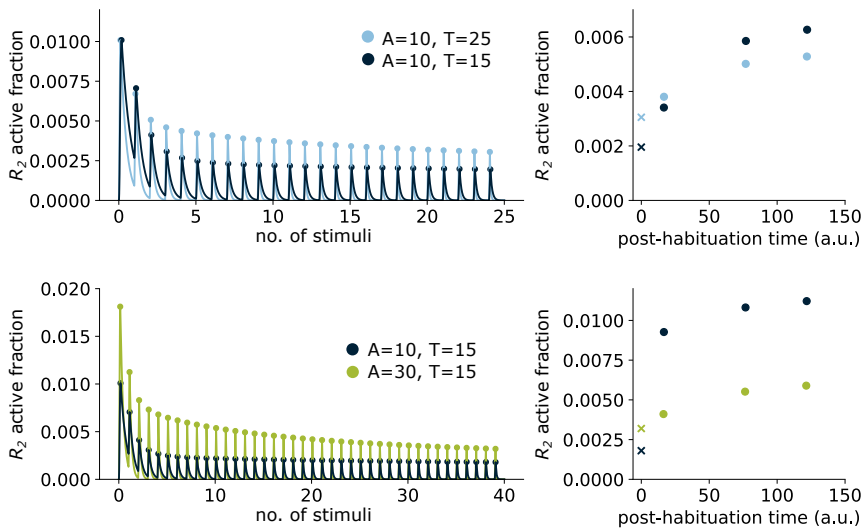


Figure 5. Frequency and intensity sensitivity for the CIFF model

This figure uses the separate test framework advocated in Colwill et al.¹⁵ and discussed in the text.

(A) The left-hand plot shows habituation to different frequencies at fixed intensity, following Figure 2B. Note that stimuli are applied until both frequencies have habituated. A test stimulus at the same intensity is then applied at different times post-habitation and the response is measured (right-hand plot). “x” marks the response at the end of habituation. The response is less with lower frequency except for shortly after habituation.

(B) The left-hand plot shows habituation to different intensities at fixed frequency, following Figure 3A, with stimulation continued until both intensities have habituated. Testing was then done as in (A) at the highest intensity of 30. The response is less with greater intensity of the habituation stimulus at all test times.

between adaptation and habituation suggests looking for network motifs that show adaptation, such as the NF, IFF, and P motifs. Random sampling of small networks has repeatedly uncovered the NF and IFF motifs,^{31,32} suggesting that there are relatively few small networks that robustly exhibit adaptation. Second, concatenation of such motifs appears to be needed to achieve frequency sensitivity. However, this hallmark also requires timescale separation, with the emergence of two memory variables that decay at markedly different timescales, which would be harder to confirm experimentally. Interventions that perturb timescale separation may still be informative, if they diminish or abolish frequency sensitivity. The NF and IFF motifs can be experimentally distinguished.⁶⁴ It would be interesting if such methods of cellular interrogation⁶⁵ could be enhanced to distinguish different molecular networks for habituation.

Two broad theories have emerged to account for habituation. The dual-process theory of Thompson and colleagues sees habituation and its counterpart, sensitization, as processes that compete with each other.⁶⁶ This competition is reflected in the IFF and NF motifs (Figures 1B and 1C), where I activates the response R , whereas M inactivates R . The response is determined by the competition between these processes. Depending on the parametric settings and the stimulation regime, we can readily find sensitization, in which the response increases with repeated stimulation. Indeed, we had to filter out sensitization to find habituation in our parametric search (STAR Methods). To put it another way, had we searched for sensitization, or for a mixture of both sensitization and habituation, we would probably have found them. Our models thereby reflect the competitive aspect of dual-process theory but without needing separate processes of habituation and sensitization.

The other broad theory, which goes back to Sokolov²⁹ and has been particularly developed by Allan Wagner,⁶⁷ sees learning as the formation of an internal representation, or memory, in which habituation may play a part, along with other forms of learning, such as conditioning, which involve multiple stimuli. The internal representation is reflected in our models by the memory variables, M_1 and M_2 . As long as M_2 is present at a non-zero level

before the recovery time has elapsed, there is a long-term memory that can be elicited through potentiation. The issue of multiple stimuli arises for hallmarks #7 to #9. It would be interesting to incorporate a wider context of multiple stimuli into our models, but this must be left to future work.

The two broad theories described above bear on a further issue mentioned in the introduction. The perspective of habituation that comes from cognitive science is rather different from that which comes from neuroscience, as expressed by Rankin et al.¹⁴ and the hallmarks in Table 1. The issues are clearly described in Colwill et al.¹⁵ The central claim from cognitive science is that the neuroscience view of habituation confuses the distinction between learning, considered as the formation of an internal representation, and performance, which elicits evidence for that representation. The internal representation of repetitive stimulation should therefore be assessed separately from the observed decline in response (Figure 1A). Older work of Wagner and colleagues on the acoustic startle response in rats is highlighted to show that, by using a separate test framework post-habitation, changes of frequency and intensity lead to opposite responses to those described in Table 1 (Figures 1B and 5 in Colwill et al.¹⁵). Here, following habituation, the system is allowed to recover for some time, and then a common test stimulus is applied across all habituating regimes. The response is found to be stronger for systems habituated under higher frequency or lower intensity, in contrast to the responses during the habituation protocol, which are weaker under higher frequency or lower intensity. Following Wagner, cognitive scientists consider the post-habitation test as more informative of the internal representation and the extent of learning that has occurred.

The relationship between learning and internal representation and the need to distinguish learning from performance seemed compelling to us.⁴⁴ We also noted that post-habitation recovery after testing for frequency sensitivity showed behavior similar to that described in Colwill et al.¹⁵ (Figure 2D). We therefore decided to test our models in the way suggested. Figure 5 shows that the CIFF model exhibits the opposite behavior described in Colwill et al.¹⁵ (frequency change shows the same behavior

shortly after habituation, but this changes subsequently). Note that in [Figure 5](#), stimulation is continued until habituation has been achieved in all conditions, whereas in [Figure 2D](#), stimulation is halted in each condition after habituation is achieved.

It is not difficult to see from our model why the behavior in [Figure 5](#) should be expected. It hinges on the level of M_2 . With frequency change at fixed intensity, M_2 is lower for higher frequency due to reversal ([Figure 2C](#)) and stays lower post-habituation, so that the test response is higher. With intensity change at fixed frequency, where there is no reversal, M_2 is higher for higher intensity ([Figure 3B](#)) and stays higher post-habituation, so that the test response is lower. This shows that, in the setting of our models for the cellular context, the discord between the two views of habituation is easily reconciled. They are both correct.

This last observation illustrates some of the benefits of studying learning in single cells. It may be simpler than in animals with central nervous systems (although our knowledge of the actual ecological complexities encountered by cells in their natural environments remains slight, at best), but this simplicity brings with it considerable benefits. We may be able to determine the underlying molecular mechanisms and understand how and why they work, as suggested by our mathematical models. Moreover, modern work in a variety of animal models has uncovered surprising complexity in the underlying mechanisms of habituation, leading one recent perspective to ask “why is the simplest form of learning so complicated?”⁶⁸ The cellular level may enable this conundrum to be more readily addressed. We hope that such opportunities will encourage others to bring cognitive science to bear on the biology of the cell.^{44,69,70} There is still much to be learned by studying learning in single cells.

RESOURCE AVAILABILITY

Lead contact

Further information and requests for resources should be directed to and will be fulfilled by the lead contact, Jeremy Gunawardena (jeremy_gunawardena@hms.harvard.edu).

Materials availability

This study did not generate new unique reagents.

Data and code availability

- The simulation data generated in this paper are available together with the code at <https://github.com/theobiolab/habituation.git> and have been deposited on Zenodo at <https://doi.org/10.5281/zenodo.14053864>.
- Any additional information required to reanalyze the data reported in this paper is available from the [lead contact](#) upon request.

ACKNOWLEDGMENTS

We thank Arjun Raj and two anonymous reviewers for their thoughtful and constructive comments. M.S.V.-S. was supported by PhD Fellowship 2021-FI-B-00408 from the Agència de Gestió d'Ajuts Universitaris i de Recerca (AGAUR) from the Generalitat de Catalunya. Z.Z. was supported by a Harvard University Program for Research in Science and Engineering (PRISE) Award. J.G.-O. was supported by the Spanish State Research Agency and FEDER Project PID2021-127311NB-I00, the Spanish Ministry of Science and Innovation, and the Generalitat de Catalunya (ICREA programme). R.M.-C. was supported by EMBO fellowship ALTF683-2019, RYC2021-033860-I funded by MCIN/AEI/10.13039/501100011033 and by the European Union NextGeneration EU/PRTR; R.M.-C. also acknowledges the support of the

Spanish Ministry of Science and Innovation through the Centro de Excelencia Severo Ochoa (CEX2020-001049-S, MCIN/AEI /10.13039/ 501100011033) and the Generalitat de Catalunya through the CERCA programme. J.G. was supported by AFOSR grant FA9550-22-1-0345. The work of M.S.V.-S., J.G.-O., and R.M.-C. was partially carried out at the Barcelona Collaboratorium for Modelling and Predictive Biology.

AUTHOR CONTRIBUTIONS

L.E., M.S.V.-S., and Z.Z. performed research; R.M.-C. and J.G. designed research; J.G.-O., R.M.-C., and J.G. supervised research. L.E., M.S.V.-S., R.M.-C., and J.G. wrote the paper with input from all authors.

DECLARATION OF INTERESTS

The authors declare no competing interests.

STAR★METHODS

Detailed methods are provided in the online version of this paper and include the following:

- [KEY RESOURCES TABLE](#)
- [METHOD DETAILS](#)
 - Mathematical models
 - Model simulations and habituation protocol
 - Parameter searching

SUPPLEMENTAL INFORMATION

Supplemental information can be found online at <https://doi.org/10.1016/j.cub.2024.10.041>.

Received: August 4, 2024

Revised: September 30, 2024

Accepted: October 14, 2024

Published: November 19, 2024

REFERENCES

1. Thompson, R.F. (2009). Habituation: a history. *Neurobiol. Learn. Mem.* 92, 127–134. <https://doi.org/10.1016/j.nlm.2008.07.011>.
2. Gagliano, M., Renton, M., Depczynski, M., and Mancuso, S. (2014). Experience teaches plants to learn faster and forget slower in environments where it matters. *Oecologia* 175, 63–72. <https://doi.org/10.1007/s00442-013-2873-7>.
3. Boisseau, R.P., Vogel, D., and Dussutour, A. (2016). Habituation in non-neural organisms: evidence from slime moulds. *Proc. Biol. Sci.* 283, 20160446. <https://doi.org/10.1098/rspb.2016.0446>.
4. Jennings, H.S. (1906). *Behavior of the Lower Organisms* (Columbia University Press).
5. McFadden, P.N., and Koshland, D.E., Jr. (1990). Habituation in the single cell: diminished secretion of norepinephrine with repetitive depolarization of PC12 cells. *Proc. Natl. Acad. Sci. USA* 87, 2031–2035. <https://doi.org/10.1073/pnas.87.5.2031>.
6. Meins, F., Jr. (1989). Habituation: heritable variation in the requirement of cultured plant cells for hormones. *Annu. Rev. Genet.* 23, 395–408. <https://doi.org/10.1146/annurev.ge.23.120189.002143>.
7. Pischke, M.S., Huttlin, E.L., Hegeman, A.D., and Sussman, M.R. (2006). A transcriptome-based characterization of habituation in plant tissue culture. *Plant Physiol.* 140, 1255–1278. <https://doi.org/10.1104/pp.105.076059>.
8. Shen, Y., Dasgupta, S., and Navlakha, S. (2020). Habituation as a neural algorithm for online odor discrimination. *Proc. Natl. Acad. Sci. USA* 117, 12402–12410. <https://doi.org/10.1073/pnas.1915252117>.

9. Gershman, S.J. (2024). Habituation as optimal filtering. *iScience* 27, 110523. <https://doi.org/10.1016/j.isci.2024.110523>.
10. Oakes, L.M. (2010). Using habituation of looking time to assess mental processes in infancy. *J. Cogn. Dev.* 11, 255–268. <https://doi.org/10.1080/15248371003699977>.
11. McDiarmid, T.A., Bernardos, A.C., and Rankin, C.H. (2017). Habituation is altered in neuropsychiatric disorders—a comprehensive review with recommendations for experimental design and analysis. *Neurosci. Biobehav. Rev.* 80, 286–305. <https://doi.org/10.1016/j.neubiorev.2017.05.028>.
12. Thompson, R.F., and Spencer, W.A. (1966). Habituation: a model phenomenon for the study of neuronal substrates of behaviour. *Psychol. Rev.* 73, 16–43. <https://doi.org/10.1037/h0022681>.
13. Pinsker, H., Kupfermann, I., Castellucci, V., and Kandel, E. (1970). Habituation and dishabituation of the gill-withdrawal reflex in *Aplysia*. *Science* 167, 1740–1742. <https://doi.org/10.1126/science.167.3926.1740>.
14. Rankin, C.H., Abrams, T., Barry, R.J., Bhatnagar, S., Clayton, D.F., Colombo, J., Coppola, G., Geyer, M.A., Glanzman, D.L., Marsland, S., et al. (2009). Habituation revisited: an updated and revised description of the behavioral characteristics of habituation. *Neurobiol. Learn. Mem.* 92, 135–138. <https://doi.org/10.1016/j.nlm.2008.09.012>.
15. Colwill, R.M., Lattal, K.M., Whitlow, J.W., Jr., and Delamater, A.R. (2023). Habituation: it's not what you think it is. *Behav. Processes* 207, 104845. <https://doi.org/10.1016/j.beproc.2023.104845>.
16. Dexter, J.P., Prabakaran, S., and Gunawardena, J. (2019). A complex hierarchy of avoidance behaviours in a single-cell eukaryote. *Curr. Biol.* 29, 4323–4329.e2. <https://doi.org/10.1016/j.cub.2019.10.059>.
17. Baluska, F., and Levin, M. (2016). On having no head: cognition throughout biological systems. *Front. Psychol.* 7, 902. <https://doi.org/10.3389/fpsyg.2016.00902>.
18. Solé, R., Moses, M., and Forrest, S. (2019). Liquid brains, solid brains. *Philos. Trans. R. Soc. Lond. B Biol. Sci.* 374, 20190040. <https://doi.org/10.1098/rstb.2019.0040>.
19. Tang, S.K.Y., and Marshall, W.F. (2018). Cell learning. *Curr. Biol.* 28, R1180–R1184. <https://doi.org/10.1016/j.cub.2018.09.015>.
20. Gershman, S.J., Balbi, P.E.M., Gallistel, C.R., and Gunawardena, J. (2021). Reconsidering the evidence for learning in single cells. *eLife* 10, e61907. <https://doi.org/10.7554/eLife.61907>.
21. Dussutour, A. (2021). Learning in single-cell organisms. *Biochem. Biophys. Res. Commun.* 564, 92–102. <https://doi.org/10.1016/j.bbrc.2021.02.018>.
22. Li, J., Ravindran, P.T., O'Farrell, A., Busch, G.T., Boe, R.H., Niu, Z., Woo, S., Dunagin, M.C., Jain, N., Goyal, Y., et al. (2024). AP-1 mediates cellular adaptation and memory formation during therapy resistance. Preprint at *bioRxiv*. <https://doi.org/10.1101/2024.07.25.604999>.
23. Vuscan, P., Kischkel, B., Joosten, L.A.B., and Netea, M.G. (2024). Trained immunity: general and emerging concepts. *Immunol. Rev.* 323, 164–185. <https://doi.org/10.1111/immr.13326>.
24. Naik, S., and Fuchs, E. (2022). Inflammatory memory and tissue adaptation in sickness and in health. *Nature* 607, 249–255. <https://doi.org/10.1038/s41586-022-04919-3>.
25. Wood, D.C. (1988). Habituation in *Stentor*: a response-dependent process. *J. Neurosci.* 8, 2248–2253. <https://doi.org/10.1523/JNEUROSCI.08-07-02248.1988>.
26. Rajan, D., Makushok, T., Kalish, A., Acuna, L., Bonville, A., Correa Almanza, K.C., Garibay, B., Tang, E., Voss, M., Lin, A., et al. (2023). Single-cell analysis of habituation in *Stentor coeruleus*. *Curr. Biol.* 33, 241–251.e4. <https://doi.org/10.1016/j.cub.2022.11.010>.
27. Bonzanni, M., Rouleau, N., Levin, M., and Kaplan, D.L. (2020). Optogenetically induced cellular habituation in non-neuronal cells. *PLoS One* 15, e0227230. <https://doi.org/10.1371/journal.pone.0227230>.
28. del Rosal, E., Alonso, L., Moreno, R., Vázquez, M., and Santacreu, J. (2006). Simulation of habituation to simple and multiple stimuli. *Behav. Processes* 73, 272–277. <https://doi.org/10.1016/j.beproc.2006.06.007>.
29. Sokolov, Y.N. (1963). *Perception and the Conditioned Reflex* (Pergamon Press).
30. Alon, U. (2006). *An Introduction to Systems Biology: Design Principles of Biological Circuits* (Chapman and Hall).
31. Ma, W., Trusina, A., El-Samad, H., Lim, W.A., and Tang, C. (2009). Defining network topologies that can achieve biochemical adaptation. *Cell* 138, 760–773. <https://doi.org/10.1016/j.cell.2009.06.013>.
32. Shi, W., Ma, W., Xiong, L., Zhang, M., and Tang, C. (2017). Adaptation with transcriptional regulation. *Sci. Rep.* 7, 42648. <https://doi.org/10.1038/srep42648>.
33. Eckert, L. (2022). *Learning in Single Cells: Computational Models of Habituation*. Master's thesis (ETH Zürich and Harvard University).
34. Staddon, J.E.R. (1993). On rate-sensitive habituation. *Adapt. Behav.* 1, 421–436. <https://doi.org/10.1177/105971239300100402>.
35. Staddon, J.E.R., and Higa, J.J. (1996). Multiple time scales in simple habituation. *Psychol. Rev.* 103, 720–733. <https://doi.org/10.1037/0033-295x.103.4.720>.
36. Friedlander, T., and Brenner, N. (2009). Adaptive response by state-dependent inactivation. *Proc. Natl. Acad. Sci. USA* 106, 22558–22563. <https://doi.org/10.1073/pnas.0902146106>.
37. Bonzanni, M., Rouleau, N., Levin, M., and Kaplan, D.L. (2019). On the generalization of habituation: how discrete biological systems respond to repetitive stimuli. a novel model of habituation that is independent of any biological system. *BioEssays* 41, e1900028. <https://doi.org/10.1002/bies.201900028>.
38. Smart, M., Shvartsman, S.Y., and Mönnigmann, M. (2024). Minimal motifs for habituating systems. *Proc. Natl. Acad. Sci. USA* 121, e2409330121.
39. Goldbeter, A., and Koshland, D.E. (1981). An amplified sensitivity arising from covalent modification in biological systems. *Proc. Natl. Acad. Sci. USA* 78, 6840–6844. <https://doi.org/10.1073/pnas.78.11.6840>.
40. Crick, F. (1984). Memory and molecular turnover. *Nature* 312, 101. <https://doi.org/10.1038/312101a0>.
41. Lisman, J.E. (1985). A mechanism for memory storage insensitive to molecular turnover: a bistable autophosphorylating kinase. *Proc. Natl. Acad. Sci. USA* 82, 3055–3057. <https://doi.org/10.1073/pnas.82.9.3055>.
42. Kandel, E.R., Klein, M., Castellucci, V.F., Schacher, S., and Goelet, P. (1986). Some principles emerging from the study of short- and long-term memory. *Neurosci. Res.* 3, 498–520. [https://doi.org/10.1016/0168-0102\(86\)90050-7](https://doi.org/10.1016/0168-0102(86)90050-7).
43. Prabakaran, S., Lippens, G., Steen, H., and Gunawardena, J. (2012). Post-translational modification: nature's escape from genetic imprisonment and the basis for cellular information processing. *Wiley Interdiscip. Rev. Syst. Biol. Med.* 4, 565–583. <https://doi.org/10.1002/wsbm.1185>.
44. Gunawardena, J. (2022). Learning outside the brain: integrating cognitive science and systems biology. *Proc. IEEE* 110, 590–612. <https://doi.org/10.1109/JPROC.2022.3162791>.
45. Vidal-Saez, M.S. (2024). *Experience-dependent Information Processing in Biological Systems*. PhD thesis (Universitat Pompeu Fabra).
46. Cornish-Bowden, A. (1995). *Fundamentals of Enzyme Kinetics, Second Edition* (Portland Press).
47. Wang, A.G., Son, M., Kenna, E., Thom, N., and Tay, S. (2022). NF- κ B memory coordinates transcriptional responses to dynamic inflammatory stimuli. *Cell Rep.* 40, 111159. <https://doi.org/10.1016/j.celrep.2022.111159>.
48. Keath, J.R., and Westhead, E.W. (2004). Factors affecting habituation of PC12 cells to ATP. *Eur. J. Biochem.* 271, 4034–4041. <https://doi.org/10.1111/j.1432-1033.2004.04341.x>.
49. Dreo, J., Liefvooghe, A., Verel, S., Schoenauer, M., Merelo, J.J., Quemy, A., Bouvier, B., and Gmys, J. (2021). *Paradiseo: from a modular framework for evolutionary computation to the automated design of metaheuristics: 22 years of Paradiseo*. Proceedings of the Genetic and Evolutionary Computation Companion Conference (New York, NY: Association for Computing Machinery), pp. 1522–1530. <https://doi.org/10.1145/3449726.3463276>.

50. Wood, D.C. (1969). Parametric studies of the response decrement produced by mechanical stimuli in the protozoan, *Stentor coeruleus*. *J. Neurobiol.* *1*, 345–360. <https://doi.org/10.1002/neu.480010309>.
51. Morimoto, B.H., and Koshland, D.E., Jr. (1991). Short-term and long-term memory in single cells. *FASEB J.* *5*, 2061–2067. <https://doi.org/10.1096/fasebj.5.7.2010059>.
52. Goelet, P., Castellucci, V.F., Schacher, S., and Kandel, E.R. (1986). The long and the short of long-term memory—a molecular framework. *Nature* *322*, 419–422. <https://doi.org/10.1038/322419a0>.
53. Wood, D.C. (1988). Habituation in *Stentor*: produced by mechanoreceptor channel modification. *J. Neurosci.* *8*, 2254–2258. <https://doi.org/10.1523/JNEUROSCI.08-07-02254.1988>.
54. Gomperts, B.D., Kramer, L.M., and Tatham, P.E.R. (2002). *Signal Transduction* (Academic Press).
55. Purcell, A.L., Sharma, S.K., Bagnall, M.W., Sutton, M.A., and Carew, T.J. (2003). Activation of a tyrosine kinase-MAPK cascade enhances the induction of long-term synaptic facilitation and long-term memory in *Aplysia*. *Neuron* *37*, 473–484. [https://doi.org/10.1016/s0896-6273\(03\)00030-8](https://doi.org/10.1016/s0896-6273(03)00030-8).
56. Nam, K.-M., Gyori, B.M., Amethyst, S.V., Bates, D.J., and Gunawardena, J. (2020). Robustness and parameter geography in post-translational modification systems. *PLoS Comp. Biol.* *16*, e1007573. <https://doi.org/10.1371/journal.pcbi.1007573>.
57. Pauly, P.J. (1981). The Loeb-Jennings debate and the science of animal behavior. *J. Hist. Behav. Sci.* *17*, 504–515. [https://doi.org/10.1002/1520-6696\(198110\)17:4<504::aid-jhbs2300170406>3.0.co;2-1](https://doi.org/10.1002/1520-6696(198110)17:4<504::aid-jhbs2300170406>3.0.co;2-1).
58. Collins, H., and Pinch, T. (1998). *The Golem. What You Should Know About Science, Second Edition* (Cambridge University Press).
59. James, W. (1890). *The Principles of Psychology, Vol. 1* (Henry Holt and Co.).
60. Ginsburg, S., and Jablonka, E. (2010). The evolution of associative learning: a factor in the Cambrian explosion. *J. Theor. Biol.* *266*, 11–20. <https://doi.org/10.1016/j.jtbi.2010.06.017>.
61. Koshland, D.E. (1980). Bacterial chemotaxis in relation to neurobiology. *Annu. Rev. Neurosci.* *3*, 43–75. <https://doi.org/10.1146/annurev.ne.03.030180.000355>.
62. Cheever, L., and Koshland, D.E., Jr. (1992). Retention of habituation in PC12 cells. *Proc. Natl. Acad. Sci. USA* *89*, 10084–10088. <https://doi.org/10.1073/pnas.89.21.10084>.
63. Bonasio, R., Tu, S., and Reinberg, D. (2010). Molecular signals of epigenetic states. *Science* *330*, 612–616. <https://doi.org/10.1126/science.1191078>.
64. Rahi, S.J., Larsch, J., Pecani, K., Katsov, A.Y., Mansouri, N., Tsaneva-Atanasova, K., Sontag, E.D., and Cross, F.R. (2017). Oscillatory stimuli differentiate adapting circuit topologies. *Nat. Methods* *14*, 1010–1016. <https://doi.org/10.1038/nmeth.4408>.
65. Estrada, J., Andrew, N., Gibson, D., Chang, F., Gnad, F., and Gunawardena, J. (2016). Cellular interrogation: exploiting cell-to-cell variability to discriminate regulatory mechanisms in oscillatory signalling. *PLoS Comput. Biol.* *12*, e1004995. <https://doi.org/10.1371/journal.pcbi.1004995>.
66. Groves, P.M., and Thompson, R.F. (1970). Habituation: a dual-process theory. *Psychol. Rev.* *77*, 419–450. <https://doi.org/10.1037/h0029810>.
67. Wagner, A.R. (1981). SOP: a model of automatic memory processing in animal behavior. In *Information Processing in Animals: Memory Mechanisms*, N.E. Spear, and R.R. Miller, eds. (Erlbaum), pp. 5–47.
68. McDiarmid, T.A., Yu, A.-J., and Rankin, C.H. (2019). Habituation is more than learning to ignore: multiple mechanisms serve to facilitate shifts in behavioural strategy. *BioEssays* *41*, e1900077. <https://doi.org/10.1002/bies.201900077>.
69. Koseska, A., and Bastiaens, P.I.H. (2017). Cell signaling as a cognitive process. *EMBO J.* *36*, 568–582. <https://doi.org/10.15252/embj.201695383>.
70. Manicka, S., and Levin, M. (2019). The Cognitive Lens: a primer on conceptual tools for analysing information processing in developmental and regenerative morphogenesis. *Philos. Trans. R. Soc. Lond. B Biol. Sci.* *374*, 20180369. <https://doi.org/10.1098/rstb.2018.0369>.
71. Virtanen, P., Gommers, R., Oliphant, T.E., Haberland, M., Reddy, T., Cournapeau, D., Burovski, E., Peterson, P., Weckesser, W., Bright, J., et al. (2020). SciPy 1.0: fundamental algorithms for scientific computing in Python. *Nat. Methods* *17*, 261–272. <https://doi.org/10.1038/s41592-019-0686-2>.
72. Ahnert, K., Mulansky, M., Simos, T.E., Psihoyios, G., Tsitouras, C., and Anastassi, Z. (2011). Odeint—solving ordinary differential equations in C++. Preprint at arXiv. <https://doi.org/10.1063/1.3637934>.
73. Keijzer, M., Merelo, J.J., Romero, G., and Schoenauer, M. (2002). *Evolving Objects: a general purpose evolutionary computation library*. *Artif. Evol.* *2310*, 829–888.

STAR★METHODS

KEY RESOURCES TABLE

REAGENT or RESOURCE	SOURCE	IDENTIFIER
Deposited data		
Software and simulation output	This paper	https://doi.org/10.5281/zenodo.14053864
Software and algorithms		
Paradiseo	Dreo et al. ⁴⁹	N/A
Scripts for running simulations and analyzing results	This paper	https://github.com/theobiolab/habituation.git

METHOD DETAILS

Mathematical models

Models are implemented as systems of ordinary differential equations (ODEs), shown below, following the reaction schemes in [Figure 1D](#) (CIFF) and [Figure 4](#) (CNF, RIFF, R3MD), and as described in the text. The dynamical variables are the active forms of each molecular species, named as in the Figures, with names signifying the “active fraction”, or the concentration of the active form, relative to the total concentration of that molecular species. We take those total concentrations to each be 1, which specifies the unit of concentration. Accordingly, the term M_1 below denotes $M_{1,a}/(M_{1,i} + M_{1,a})$. Unless indicated otherwise, subscripts 1 and 2 refer to the respective motifs in the model, k_i are the reaction rates, and K_i are the Michaelis-Menten constants, again normalised to the total concentration of the corresponding substrate. The repetitive stimulus ([Figure 1A](#)) is denoted by $SQW(t)$. We use \dot{x} to stand for dx/dt .

CIFF model, [Figure 1D](#):

$$\dot{I}_1 = SQW(t) \times k_{Ia1}(1 - I_1) - k_{Ii1}I_1$$

$$\dot{M}_1 = I_1 \times k_{Ma1}(1 - M_1) - k_{Mi1}M_1$$

$$\dot{R}_1 = I_1 \times k_{Ra1}(1 - R_1) - M_1 k_{Ri1} \frac{R_1}{K_1 + R_1}$$

$$\dot{I}_2 = R_1 \times k_{Ia2}(1 - I_2) - k_{Ii2}I_2$$

$$\dot{M}_2 = I_2 \times k_{Ma2}(1 - M_2) - k_{Mi2}M_2$$

$$\dot{R}_2 = I_2 \times k_{Ra2}(1 - R_2) - M_2 k_{Ri2} \frac{R_2}{K_2 + R_2}$$

CNF model, [Figure 4A](#):

$$\dot{I}_1 = SQW(t) \times k_{Ia1}(1 - I_1) - k_{Ii1}I_1$$

$$\dot{M}_1 = R_1 \times k_{Ma1}(1 - M_1) - k_{Mi1}M_1$$

$$\dot{R}_1 = I_1 \times k_{Ra1}(1 - R_1) - M_1 k_{Ri1} \frac{R_1}{K_1 + R_1}$$

$$\dot{I}_2 = R_1 \times k_{Ia2}(1 - I_2) - k_{Ii2}I_2$$

$$\dot{M}_2 = R_2 \times k_{Ma2}(1 - M_2) - k_{Mi2}M_2$$

$$\dot{R}_2 = I_2 \times k_{Ra2}(1 - R_2) - M_2 k_{Ri2} \frac{R_2}{K_2 + R_2}$$

RIFF model, [Figure 4B](#):

$$\dot{P}_r = k_a P_a - k_r P_r$$

$$\dot{P}_i = k_r P_r - \text{SQW}(t) \times k_i P_i$$

$$\dot{P}_a = \text{SQW}(t) \times k_i P_i - k_a P_a$$

$$\dot{I}_2 = P_a \times k_{Ia2}(1 - I_2) - k_{Ii2}I_2$$

$$\dot{M}_2 = I_2 \times k_{Ma2}(1 - M_2) - k_{Mi2}M_2$$

$$\dot{R}_2 = I_2 \times k_{Ra2}(1 - R_2) - M_2 k_{Ri2}R_2$$

R3MD model, [Figure 4C](#).

$$\dot{P}_r = k_a P_a + k_{FB} M_2 P_a - k_r P_r$$

$$\dot{P}_i = k_r P_r - \text{SQW}(t) \times k_i P_i$$

$$\dot{P}_a = \text{SQW}(t) \times k_i P_i - k_{FB} k_a P_a$$

$$\dot{I}_2 = P_a \times k_{Ia2}(1 - I_2) - k_{Ii2}I_2$$

$$\dot{R}_2 = I_2 \times k_{Ra2}(1 - R_2) - k_{Ri2}R_2$$

$$\dot{M}_2 = R_2 \times k_{Ma2}(1 - M_2) - k_{Mi2}M_2$$

Model simulations and habituation protocol

We numerically integrated the ODEs described above in both Python and C++, to cross-check the accuracy of the solutions. In Python, we used the `odeint` routine from Scipy.⁷¹ In C++, we used the `runge_kutta4` function from Boost's `odeint` library,⁷² which we executed with a step size of 0.001. We assume the model starts with all species inactive. In order to reduce numerical inaccuracies that can arise because of the discontinuous nature of $\text{SQW}(t)$ ([Figure 1A](#)) the time intervals in which the stimulus was on or off were integrated consecutively, using the final values of the preceding time interval as the initial conditions for the next interval. In Python, for each interval, integration was initially performed with a relatively large maximum step size of 10^{-2} which was successively lowered down to 10^{-6} in case of integration failure.

As explained in the main text, we developed an algorithm to extract the sequence of peaks and troughs of the simulation output as local maxima and minima, respectively, of the trajectory of the output response. We then filtered the sequence of peaks and troughs to identify habituating trajectories. The filter conditions, listed below, were developed after substantial trial and error exploration to rule out various unusual trajectories.

- 1) The array of peaks must not be empty.
- 2) The highest peak must not be found later than the third position. This allows for some sensitisation for the very first stimuli ([discussion](#)).
- 3) The first peak must not be much lower than the highest peak: the former should not be less than 50% of the latter.
- 4) All peaks after the highest peak must be monotonically decreasing.
- 5) There must be at least two peaks after the highest peak.
- 6) There must be a substantial difference between the highest and the lowest peak: the latter should be no more than 80% of the former.
- 7) There must be a substantial peak to trough difference for the first few peaks, with the relative difference, normalised to the maximum peak height, satisfying

$$\frac{\text{peak} - \text{trough}}{\max(\text{peak})} > 0.05.$$

This excludes dynamical trajectories that are too smoothly varying.

- 8) Troughs must not be too high: not higher than 60% of the highest peak.
- 9) The last trough must be almost zero: not higher than 2% of the highest peak.
- 10) The number of high troughs should be limited, with no more than 5 troughs being higher than 10% of the highest peak.

At each stimulus, we tested whether or not the system had habituated, as explained in the main text, and, if it had, we terminated simulation at that point. We rejected parameter sets that did not habituate within 50 stimuli. The results shown in the paper and the [supplemental information](#) were obtained in both Python and C++ to double check the habituation (*ht*) and recovery times (*rt*).

Parameter searching

Given a model, we were able to identify a region of parameter space in which habituation typically occurs. To do this, we first manually located parameter ranges in which habituation sometimes occurred. We then took pairs of parameters and iteratively constrained their corresponding ranges so that habituation progressively occurred with greater frequency. After some exploration, we were able to identify parameter ranges in which habituation typically occurred. The corresponding ranges are shown for each model in [Table S1](#) (CIFF), S2 (CNF), S3 (RIFF) and S4 (R3MD).

We exploited the habituating region of parameter space to find parameter sets that exhibit frequency and intensity sensitivity. To do this, we minimised the cost function described in [Equation 1](#), using ParadisEO,⁴⁹ an object-oriented framework for designing meta-heuristics for evolutionary optimisation, based on the Evolving Objects (EO) C++ library.⁷³ We used the evolution strategy with self-adaptive mutation algorithm offered by ParadisEO. This algorithm is executed through a C++ source-code file, ESEA.cpp, in which cost-function values evaluated by our C++ code are made available for optimisation. The algorithm broadly works as follows; for more details see Lesson 4 of the tutorial on the EO website at eodev.sourceforge.net. We used default settings for the hyperparameters, except for the population size, which we set to 10 to reduce the overhead of cost-function calculation. An initial population of 10 “genotypes” was selected by independently choosing parameter values from the uniform distributions on the ranges. An additional parameter, which will be treated as the standard deviation, *s*, of a normal distribution $\mathcal{N}(m, s)$ with mean *m*, was added to each genotype with initial value $s = 0.3$. It is this genotype extension that makes the algorithm “self adaptive”. Two parents were selected by randomly choosing two pairs of genotypes and selecting in each pair the genotype with the lowest cost-function value. Two children were generated from the two parents by a combination of “crossover”, which happens with probability 0.6, followed by “mutation”, which happens with probability 0.1. Crossover merely exchanges the actual parameter values, while the two standard deviations, *s*₁ and *s*₂, are replaced by two random points in the interval between them: $\alpha s_1 + (1 - \alpha)s_2$, where α is drawn independently from the uniform distribution on [0, 1]. The actual parameters were mutated by replacing each value with another drawn from $\mathcal{N}(p, s)$, where *p* is the parameter value and *s* is the standard deviation of that genotype. The standard deviation, *s*, of each genotype was mutated to $s \exp(a)$, where *a* is randomly drawn from $\mathcal{N}(0, 1)$. This process was repeated with more parents to generate a new population of 10 children. The algorithm was run for 200 generations. The lowest-cost parameter sets are shown in [Tables S1](#) (CIFF), S2 (CNF), S3 (RIFF) and S4 (R3MD).

Current Biology, Volume 34

Supplemental Information

**Biochemically plausible models of habituation
for single-cell learning**

Lina Eckert, Maria Sol Vidal-Saez, Ziyuan Zhao, Jordi Garcia-Ojalvo, Rosa Martinez-Corral, and Jeremy Gunawardena

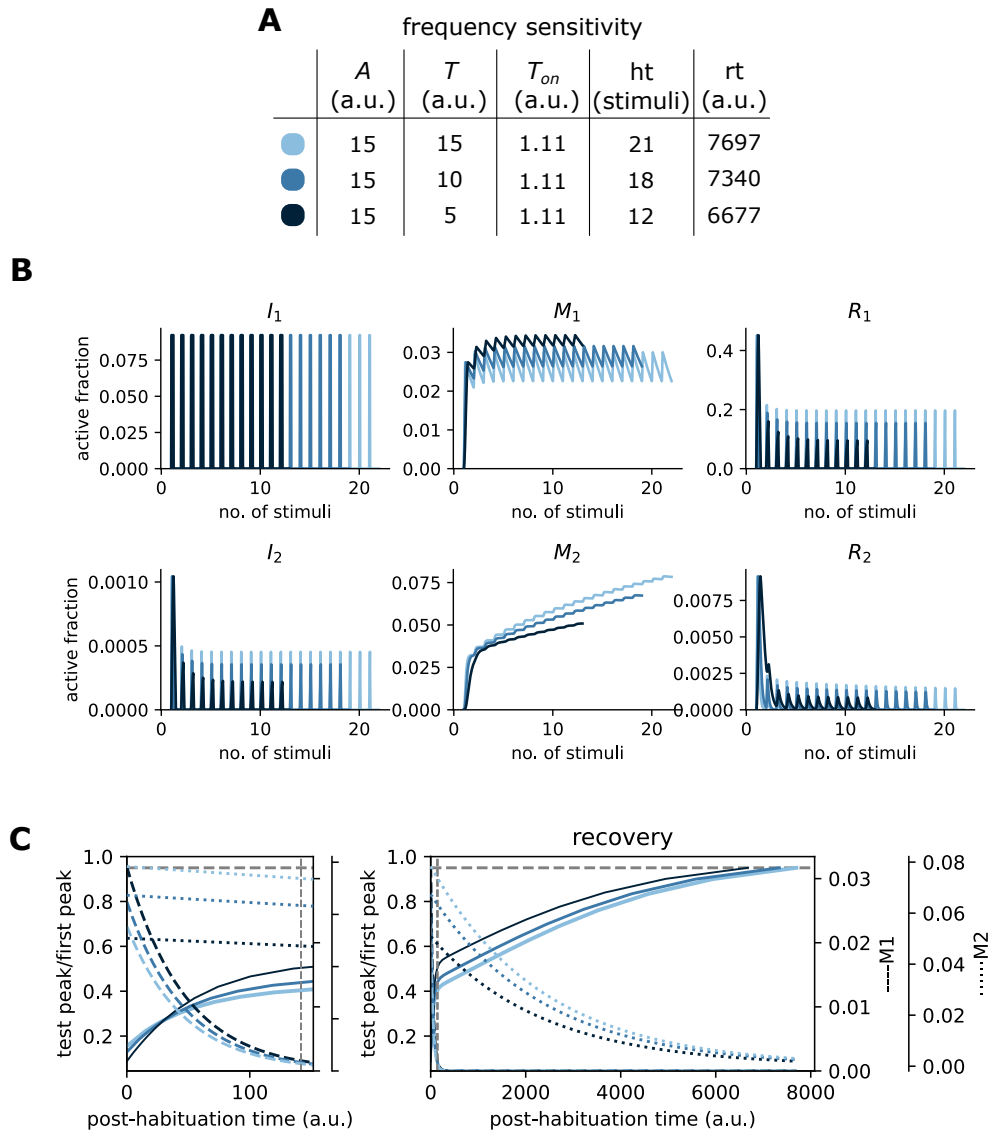


Figure S1: Frequency sensitivity for the CNF model in Figure 4A. Related to Figure 4. The panels are organized as described in Figure 2. The corresponding parameter set is given in Table S2.

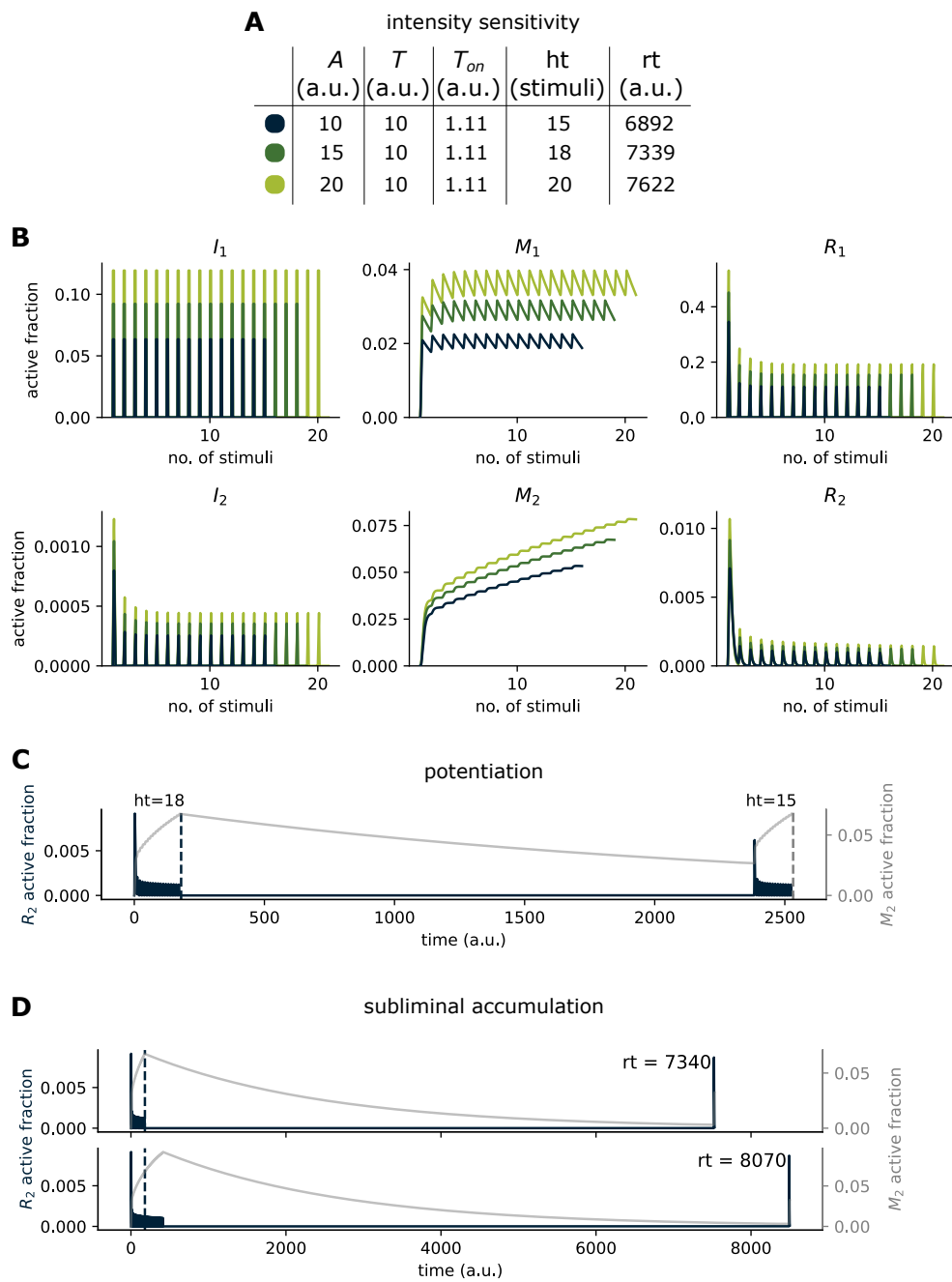


Figure S2: Intensity sensitivity, potentiation and subliminal accumulation for the CNF model in Figure 4A. Related to Figure 4. The panels are organized as described in Figure 3. The corresponding parameter set is given in Table S2.

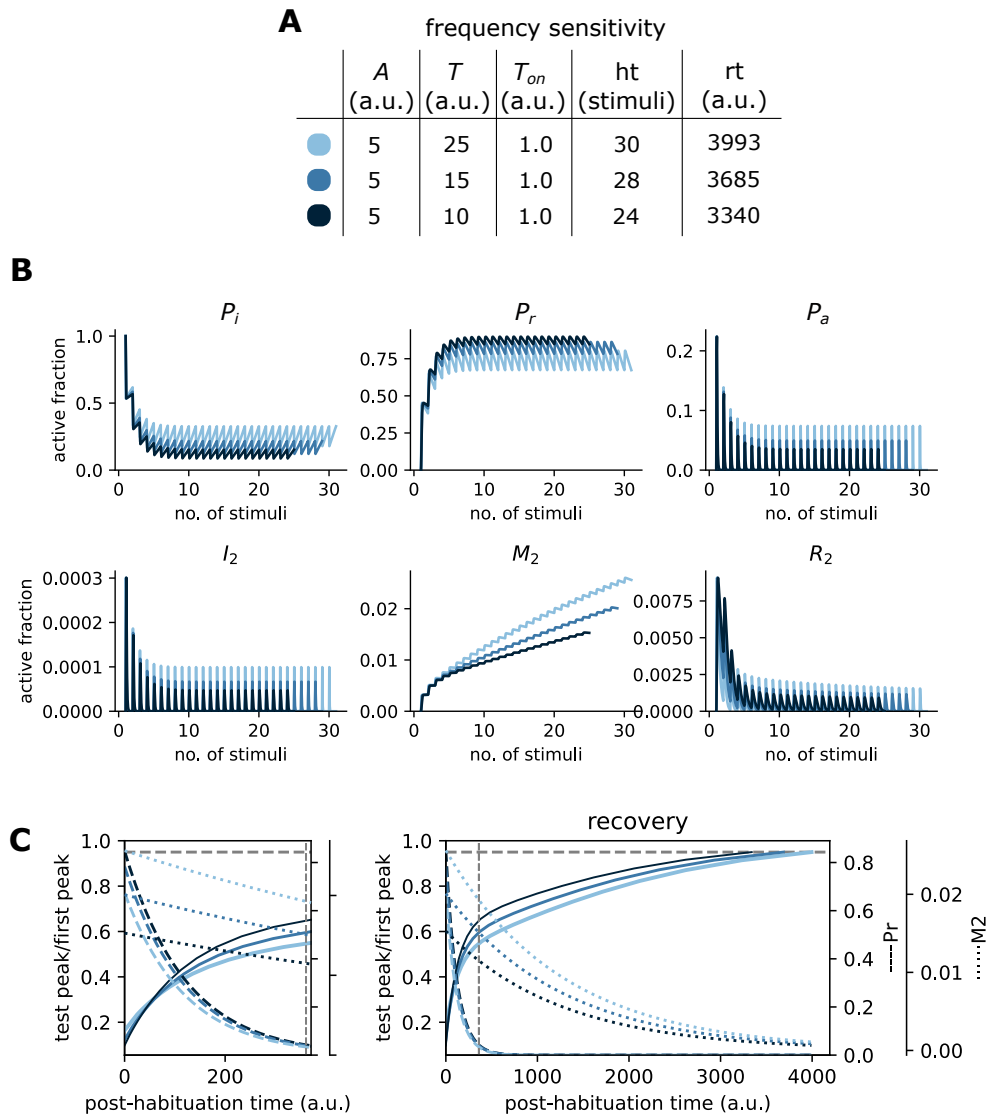


Figure S3: Frequency sensitivity for the RIFF model in Figure 4B. Related to Figure 4. The panels are organized as described in Figure 2. The corresponding parameter set is given in Table S3.

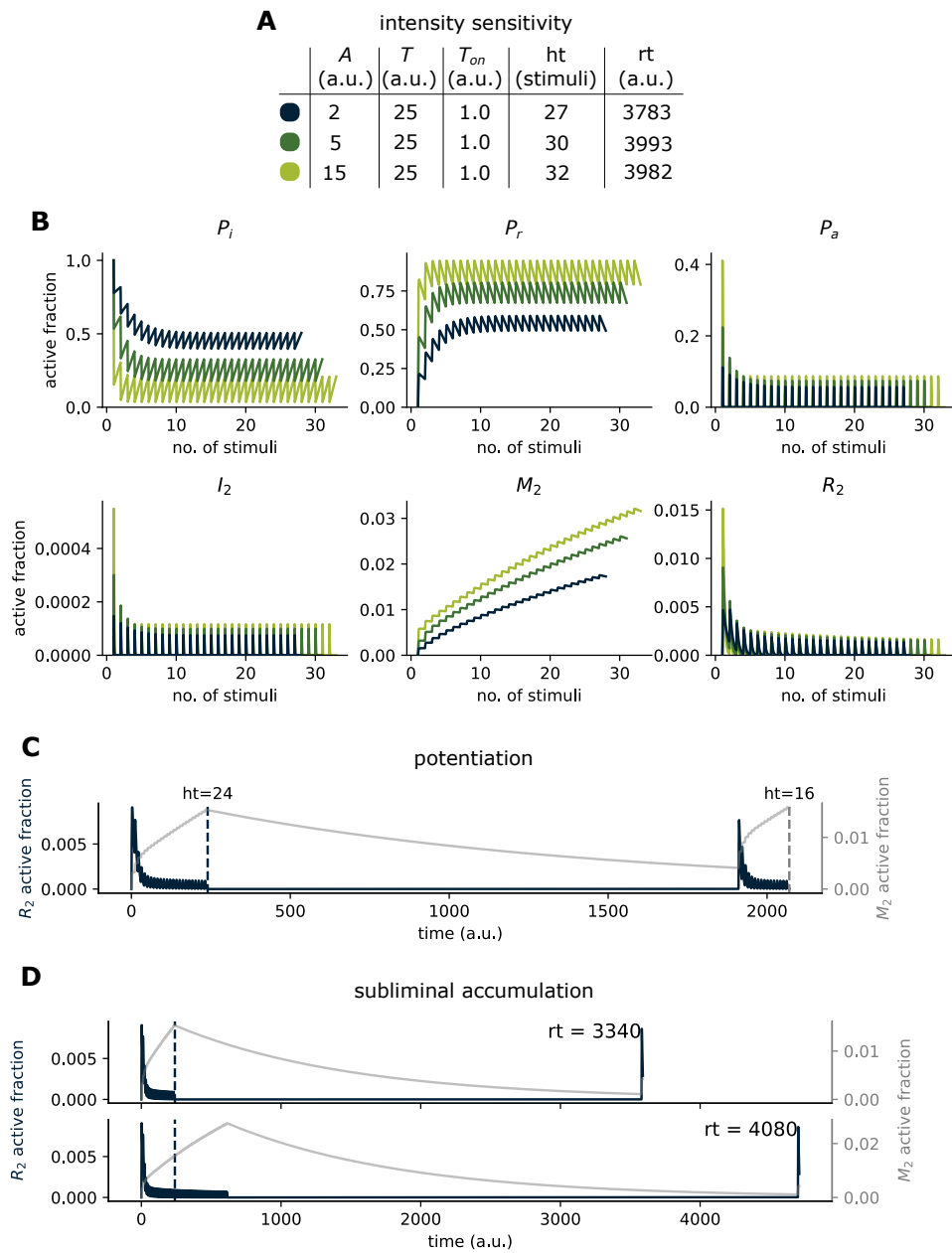


Figure S4: Intensity sensitivity, potentiation and subliminal accumulation for the RIFF model in Figure 4B. Related to Figure 4. The panels are organized as in Figure 3. The corresponding parameter set is given in Table S3.

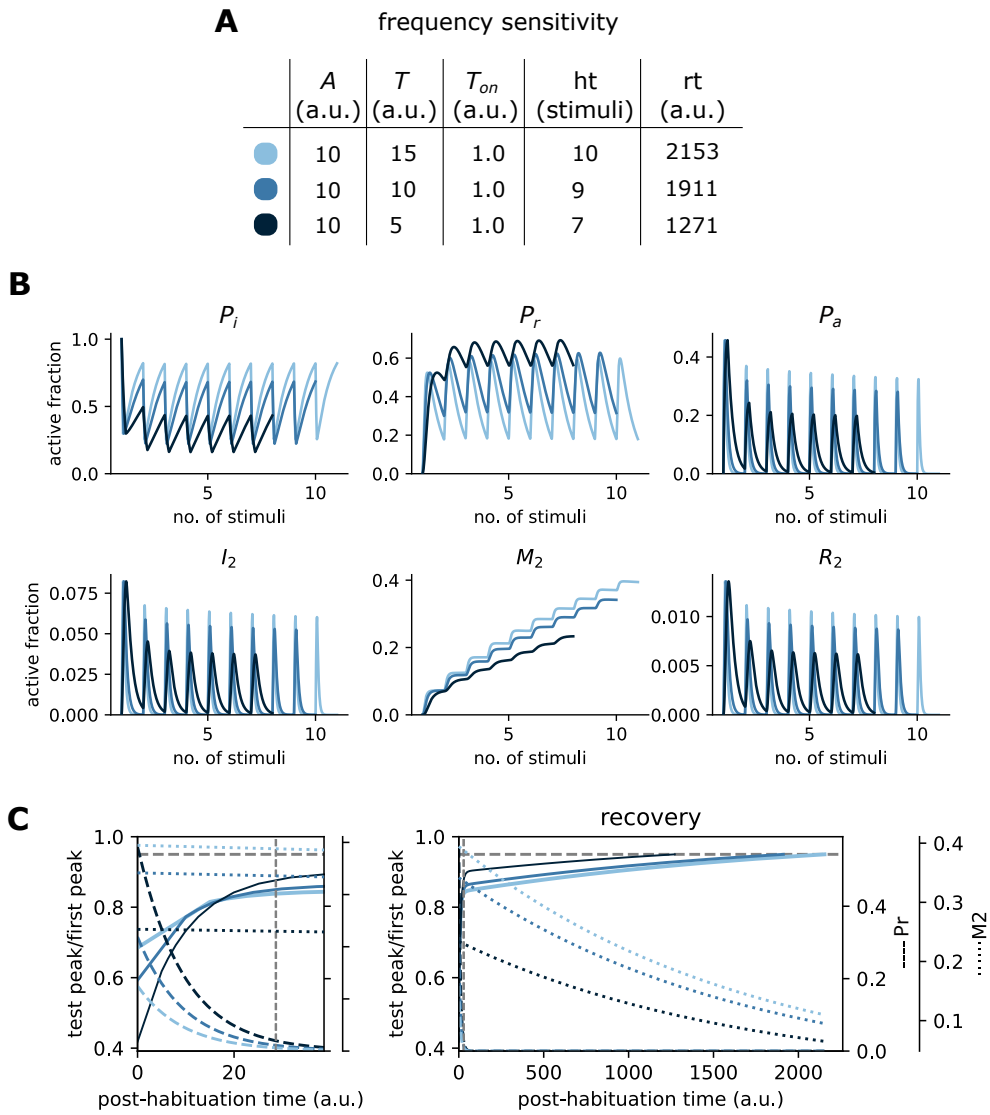


Figure S5: Frequency sensitivity for the R3MD model in Figure 4C. Related to Figure 4. The panels are organized as described in Figure 2. The corresponding parameter set is given in Table S4.

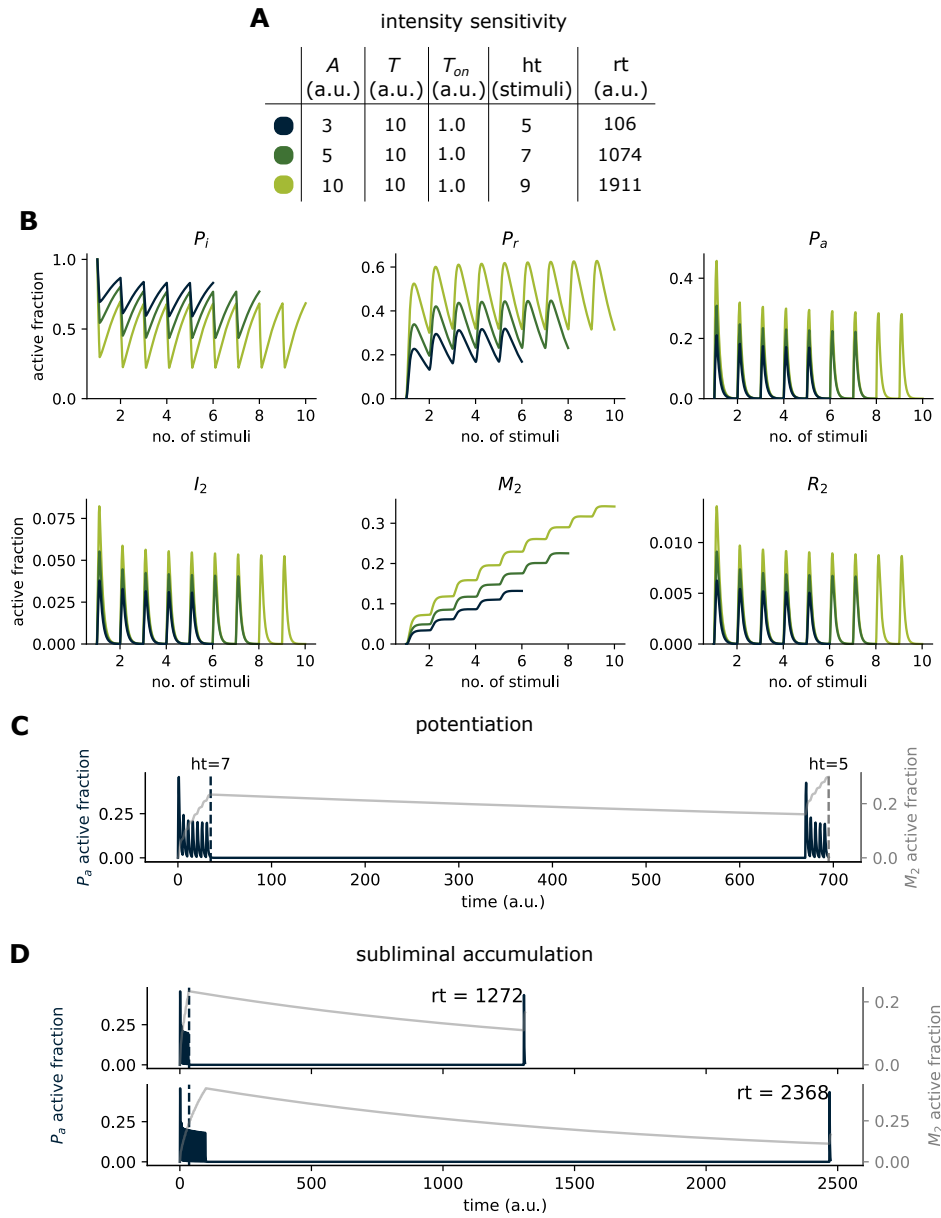


Figure S6: Intensity sensitivity, potentiation and subliminal accumulation for the R3MD model in Figure 4C. Related to Figure 4. The panels are organized as described in Figure 3. The corresponding parameter set is given in Table S4.

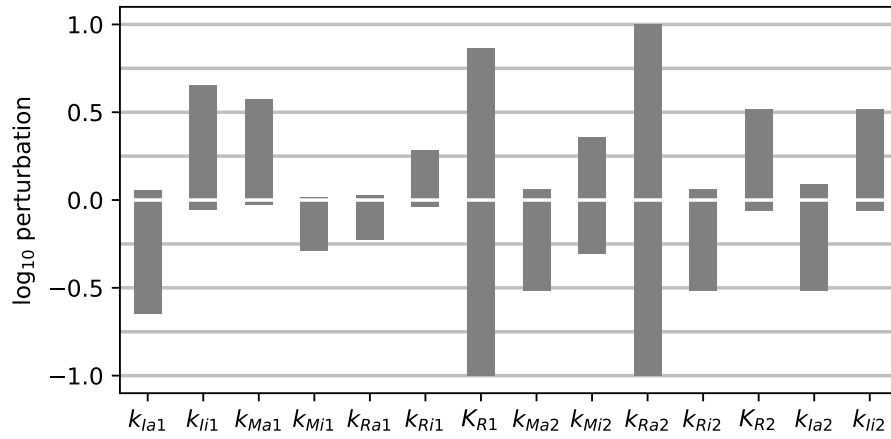


Figure S7: Sensitivity analysis for the CIFF model in Figure 1D. Related to Figure 1. The corresponding parameter set, whose values give the baseline for the perturbations, is shown in Table S1. See the Methods for details.

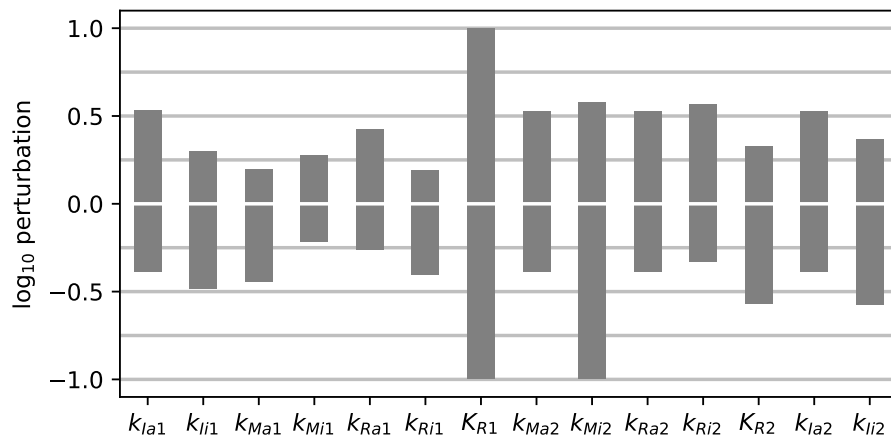


Figure S8: Sensitivity analysis for the CNF model in Figure 4A. Related to Figure 4. The corresponding parameter set, whose values give the baseline for the perturbations, is shown in Table S2. See the Methods for details.

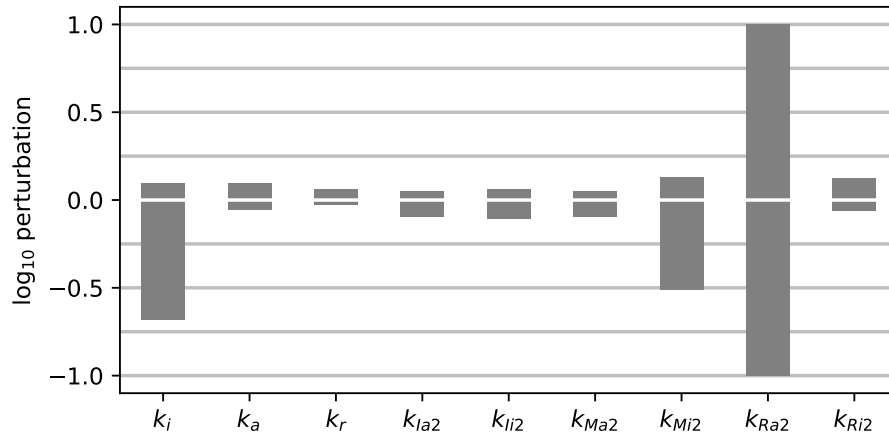


Figure S9: Sensitivity analysis for the RIFF model in Figure 4B. Related to Figure 4. The corresponding parameter set, whose values give the baseline for the perturbations, is shown in Table S3. See the Methods for details.

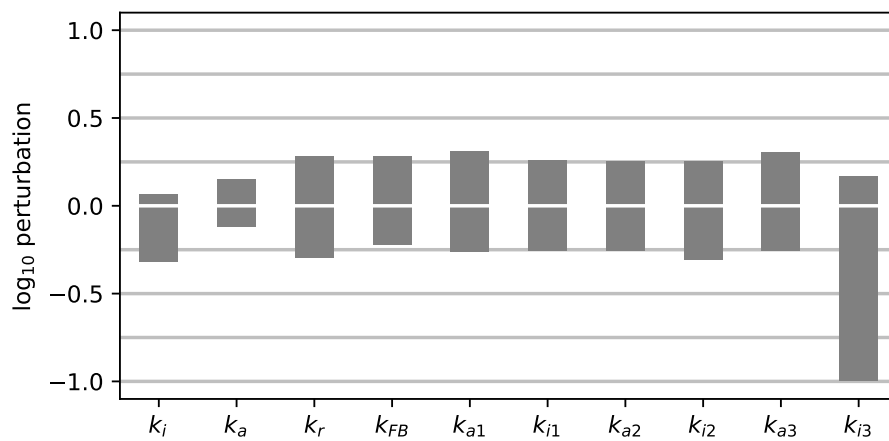


Figure S10: Sensitivity analysis for the R3MD model in Figure 4C. Related to Figure 4. The corresponding parameter set, whose values give the baseline for the perturbations, is shown in Table S4. See the Methods for details.

Parameter	Search range	Best solution
k_{Ia1}	[0.01; 0.25]	0.023
k_{Ii1}	[30.0; 50.0]	34.44
k_{Ma1}	[8.0; 20.0]	17.71
k_{Mi1}	[0.01; 0.1]	0.0382
k_{Ra1}	[57.0; 80.0]	57.92
k_{Ri1}	[1.00; 2.10]	1.39
K_1	[0.00025; 0.002]	0.000534
k_{Ia2}	[0.012; 0.12]	0.0160
k_{Ii2}	[0.873; 20.0]	14.3
k_{Ma2}	[2.52; 20.0]	4.34
k_{Mi2}	[0.001; 0.01]	0.00147
k_{Ra2}	[1.976; 49.7]	26.2
k_{Ri2}	[12.77; 49.7]	45.99
K_2	[0.75; 2.0]	0.791

Table S1: Parameter values of the CIFF model in Figure 1D for the stimulation regimes shown in Figures 2B and 3A. Related to Figures 2 and 3.

Parameter	Search range	Best solution
k_{Ia1}	[0.0225; 0.0235]	0.023
k_{Ii1}	[30.0; 50.0]	33.97
k_{Ma1}	[0.04; 0.076]	0.049
k_{Mi1}	[0.02; 0.046]	0.0211
k_{Ra1}	[5.80; 15.90]	7.74
k_{Ri1}	[15.40; 35.50]	18.19
K_1	[0.00025; 0.002]	0.000691
k_{Ia2}	[0.03; 0.06]	0.0373
k_{Ii2}	[14.0; 37.0]	15.94
k_{Ma2}	[0.5; 2.03]	1.026
k_{Mi2}	[0.00014; 0.0018]	0.000423
k_{Ra2}	[4.71; 18.8]	7.51
k_{Ri2}	[12.77; 49.7]	22.39
K_2	[0.5; 1.58]	1.147

Table S2: Parameter values of the CNF model in Figure 4A for the stimulation regimes shown in Figures S1A and S2A. Related to Figures 4, S1 and S2.

Parameter	Search range	Best solution
k_a	[0.1; 5.0]	1.497
k_r	[0.001; 0.01]	0.00830
k_i	[0.01; 1.0]	0.1255
k_{Ia2}	[0.012; 0.12]	0.01519
k_{Ii2}	[0.1; 20.0]	11.20
k_{Ma2}	[2.52; 20.0]	7.65
k_{Mi2}	[0.0001; 0.01]	0.00079
k_{Ra2}	[1.976; 49.7]	25.96
k_{Ri2}	[12.77; 49.7]	36.52

Table S3: Parameter values of the RIFF model in Figure 4B for the stimulation regimes in Figures S3A and S4A. Related to Figures 4, S3 and S4.

Parameter	Search range	Best solution
k_a	[0.1; 5.0]	0.773
k_r	[0.01; 0.5]	0.1046
k_i	[0.01; 1.0]	0.1236
k_{FB}	[0.01; 1.0]	0.9039
k_{Ia2}	[0.012; 1.5]	1.033
k_{Ii2}	[0.1; 20.0]	5.046
k_{Ra2}	[0.1; 2.0]	1.002
k_{Ri2}	[0.1; 10.0]	5.757
k_{Ma2}	[1.0; 5.0]	2.52
k_{Mi2}	[0.0001; 0.001]	0.000594

Table S4: Parameter values of the R3MD model in Figure 4C for the stimulation regimes in Figures S5A and S6A. Related to Figures 4, S5 and S6.

#	Hallmarks	Stimulus	Comments
1	Habituation	K ⁺ S1,S2 ACh ^{S2,S3,S4} ATP ^{S4,S5}	
2	Spontaneous recovery	K ⁺ S1 ACh ^{S2,S3,S4} ATP ^{S4}	Only partial recovery. Only partial recovery.
3	Potentiation of habituation	K ⁺ S1 ACh ^{S2,S3,S4} ATP ^{S4}	
4	Frequency sensitivity	K ⁺ S1 ACh ^{S3} ATP ^{S5}	Stronger habituation for higher frequencies. Recovery was not tested. Data has been normalized. Normalized data. Peaks have not fully habituated. Recovery was not tested. Normalized data. Peaks have not fully habituated. For higher frequencies habituation is more pronounced and more rapid. Recovery was not tested.
5	Intensity sensitivity	ATP ^{S5}	Normalized data (Figure 1). Indirect evidence by analogy between habituation and adaptation (Figure 3).
6	Subliminal accumulation		Not reported.
7	Stimulus specificity	K ⁺ / ACh ^{S2,S3} ATP / K ⁺ S5	Independent habituation. Stimulus generalization.
8	Dishabituation	K ⁺ S1 ACh ^{S3}	Bay K8644 and phorbol esters used as dishabituating stimuli. Phorbol esters do NOT result in dishabituation to ACh stimuli.
9	Habituation of dishabituation		Not reported.
10	Long-term habituation		Not reported.

Table S5: Summary of Koshland's work on habituation of noradrenaline secretion to multiple stimuli in PC12 cells. Tested stimuli were acetylcholine (ACh), adenosine triphosphate (ATP) and ionic potassium (K⁺). Adapted with permission from Table 6 of citation^{S6} and related to Table 1.

Supplemental references

- S1. P. N. McFadden and D. E. Koshland Jr. Habituation in the single cell: diminished secretion of norepinephrine with repetitive depolarization of PC12 cells. *Proc. Natl. Acad. Sci. USA*, 87:2031–5, 1990.
- S2. B. H. Morimoto and D. E. Koshland Jr. Short-term and long-term memory in single cells. *FASEB J.*, 5:2061–7, 1991.
- S3. P. N. McFadden and D. E. Koshland Jr. Parallel pathways for habituation in repetitively stimulated PC12 cells. *Neuron*, 4:615–21, 1990.
- S4. L. Cheever and D. E. Koshland Jr. Retention of habituation in PC12 cells. *Proc. Natl. Acad. Sci. USA*, 89:10084–8, 1992.
- S5. L. Cheever and D. E. Koshland Jr. Habituation of neurosecretory responses to extracellular ATP in PC12 cells. *J. Neurosci.*, 14:4831–8, 1994.
- S6. L. Eckert. Learning in Single Cells: Computational Models of Habituation. Master's thesis, ETH Zürich and Harvard University, 2022.